NWP SAF

Satellite Application Facility
for Numerical Weather Prediction

Document NWPSAF-MF-UD-001

Version 8.1 October 2019

AAPP DOCUMENTATION

SCIENTIFIC DESCRIPTION

Tiphaine Labrot (Météo-France)

Lydie Lavanant (Météo-France)

Keith Whyte (Met Office)

Nigel Atkinson (Met Office)

Pascal Brunel (Météo-France)

NWP SAF	AAPP DOCUMENTATION SCIENTIFIC DESCRIPTION	Doc ID : NWPSAF-MF-UD-001 Version : 8.1 Date : October 2019

This documentation was developed within the context of the EUMETSAT Satellite Application Facility on Numerical Weather Prediction (NWP SAF), under the Cooperation Agreement dated 01 December 2006, between EUMETSAT and the Met Office, UK, by one or more partners within the NWP SAF. The partners in the NWP SAF are the Met Office, ECMWF, DWD and Météo France.

Change record			
Version	Date	Author / changed by	Remarks
4.0	April 03	T.Labrot	Version1 of the scientific description document of AAPP V4.0 (Follow the version of AAPP V3.0)
4.1	12 May 2003	K. Whyte	Add references to monitoring files in section 5.3
5.0	April 2005	T.Labrot With N.Atkinson And P.Brunel	Update for AAPP version 5.0
6.0	June 2006	T.Labrot N Atkinson	Update for AAPP version 6.0
7.0	October 2011	N Atkinson	Update for AAPP version 7.0
8.0	Dec 2017	N Atkinson	Update for AAPP version 8.0
8.1	Oct 2019	N Atkinson	Provide more detail in sections 8.5.1 (AMSU scattering index) and 8.5.5 (IASI cloud tests)

TABLE OF CONTENTS

FIGURES

TABLES

1. INTRODUCTION

For many years the NOAA polar orbiting weather satellites have provided a sounding and imaging capability, with instruments operating in the visible, infra-red and microwave regions of the spectrum, and with a direct broadcast system to allow users access to the data in near real time.

In response to requests from the user community, EUMETSAT took the initiative in 1992 to start activities in the area of ATOVS software processing. The goal was to set up a standard package for the processing of locally received ATOVS data from the NOAA spacecraft, and as a result of this initiative the ATOVS and AVHRR Pre-processing Package (AAPP) was developed. The package is now maintained by the EUMETSAT Satellite Application Facility for Numerical Weather Prediction (NWP SAF).

The first satellite in the NOAA-KLM series (NOAA-15) was launched in 1998, replacing the earlier NOAA/TIROS-N series. In 2005 the first satellite in the follow-on NOAA-NN' series was launched (NOAA-18), and the AAPP package (version 5) was extended to accept data from this series.

The next major development was the launch in 2006 of the first European MetOp satellite. MetOp is part of the EUMETSAT Polar System (EPS), which is the European contribution to a joint European-US polar satellite system called the Initial Joint Polar System (IJPS). MetOp capability was added in AAPP v6. The ability to process imager data from the Chinese FY-1D satellite was also added as part of AAPP v6.

The first of the next generation of US operational polar-orbiting weather satellites is the Suomi National Polar-orbiting Partnership (Suomi-NPP), launched in October 2011. Future satellites in the series will be named JPSS (Joint Polar Satellite System). AAPP v7 was designed to pre-process data from the sounder and imager instruments on NPP, while continuing to support MetOp and the older NOAA satellites.

A number of enhancements were made to AAPP v7 during its release history, including the addition of MAIA4 to provide a cloud mask for VIIRS, the ability to ingest data from the microwave and infrared sounders on the FY-3 series of satellites, and the ability to create hdf5 output files as an alternative to traditional AAPP level 1c.

For AAPP v8, there are two major changes: the extension of MAIA4 to cover AVHRR as well as VIIRS, and interfaces to the new ecCodes BUFR/GRIB library from ECMWF.

This document provides a scientific description of the AAPP package.

2. DOCUMENTS AND TERMINOLOGY

2.1. APPLICABLE AND REFERENCE DOCUMENTS

[1]: NESS 107: 'Data Extraction and Calibration of TIROS-N/NOAA Radiometer'. NOAA Technical Memorandum - Planet, 1988.

And the NOAA KLM user's guide on the web site http://www2.ncdc.noaa.gov/docs/klm/

[2]: 'General specifications for the AAPP preprocessing package related to NOAA polar orbiting weather satellites. Scientific part'. Météo France internal document- 1999.

[3]: 'General specifications for the AAPP preprocessing package related to NOAA polar orbiting weather satellites. Software description'. Météo France internal document - 1999.

[4]: 'AAPP Module Design' - 'AAPP Data Set Definition'. Documentation EUMETSAT - Vol1 et Vol2 - 1997.

[5]: Hewison T. J. & Saunders R., 'Measurement of the AMSU-B Antenna Pattern'. *IEEE Transactions of Geosciences and Remote Sensing*, Vol. 34 No 2, Mars 1996.

[6]: Crosby, Ferraro & Wu, 'Estimating the probability of rain in an SSM/I FOV using logistic regression'. *Journal of Applied Met*., Vol 34 No 11, 1995.

[7]: Ardouin L., G. Monnier, L. Lavanant, 'Adjustment, validation and implantation of MAIA2 in AAPP software'. Technical report,1999.

[8]: Derrien D., B. Farki. L. Harang, H. LeGléau, A. Noyalet, D. Pohic, A. Sairouni, 'Automatic Cloud Detection Applied to NOAA-11/AVHRR Imagery'. *Remote Sens. Envion*. 46 :246-267, 1993.

[9]: Derrien D., & H. LeGléau, 'Cloud classification extracted from AVHRR and GOES imagery'. Proceedings of Eumetsat Meteorological satellite data conference - 1999.

[10]: Grody N., 'Classification of snow cover and precipitation using the Special Sensor Microwave Imager'. *J. Geophys. Res.*, vol 96, 1999.

[11]: Gutman G., D. Tarpley,A. Ignatov, S. Olson, 'The enhanced NOAA global dataset from the advanced very high resolution radiometer'. *Bulletin of the American Meteorological Society.* 1995.

[12]: Lavanant L., H. LeGléau, M. Derrien, S. Levasseur, G. Monnier, L. Ardouin, P. Brunel, B. Bellec, AVHRR Cloud Mask for Sounding Applications. ITSC-10 proceedings, 1999.

[13]: Oort A., Global Atmospheric Circulation Statistics. 1958 –1973.

[14]: Saunders R., 'An automated scheme for the removal of cloud contamination from AVHRR radiances over western Europe'. *Int. J. Remote sensing,* 1986.

[15]: Saunders R., 'An improved method for detecting clear sky and cloudy radiances from AVHRR data'. *Int. J. Remote Sensing*, 1988.

[16]: MAIA software documentation, version 2.1, 1999.

[17]: Brunel P. and Marsouin A., 'Operational AVHRR navigation results', *International Journal of Remote Sensing*, Vol. 21, No. 5, 951-972, 2000.

[18]: Rosborough G.W., Baldwin D. and Emery W., 'Precise AVHRR Image Navigation', *IEEE Transactions on Geoscience and Remote Sensing*, Vol. 32, No. 3, May 1994, 644-657, 1994.

[19]: Level 1B Notices, http://www.osdpd.noaa.gov/PSB/PPP/notices/notices.html

[20]: Brunel P. and Marsouin A., ANA-3 User's Manual, Meteo-France/DP/Centre de Meteorologie Spatiale, BP 147, 22302 Lannion, France, 2001.

[21]: Bordes Ph., Brunel P. and Marsouin A., 'Automatic Adjustment of AVHRR Navigation', *Journal of Atmospheric and Oceanic Technology*, Vol. 9, No. 1, 1992.

[22]: Marsouin A., Brunel P., AAPP Documentation, Annex of scientific description, AAPP-5 navigation

[23]: Changyong Cao, NESDIS, HIRS Calibration Algorithm Version 4.0

[24]: Changyong Cao and Pubu Ciren, Operational High Resolution Infrared Radiation Sounder (HIRS) Calibration Algorithms and Their Effects on Calibration Accuracy, ITSC XIII Proceedings (2003), cimss.ssec.wisc.edu/itwg/itsc/itsc13/session3/3_2_ciren.pdf

[25]: Bennartz, Thoss, Dybbroe and Michelson, 'Precipitation analysis using the Advanced Microwave Souunding Unit in support of nowcasting applications', *Meteorol. Appl.*, 9, 177-189, 2002

[26]: Lee, A.C.L. and Bedford, S., 'Support Study on IASI Level 1c Data Compression', Final Report, EUMETSAT Contract EUM/CO/-3/1155/PS, Feb 27, 2004

[27]: Goldberg et. al., "AIRS Near-Real-Time Products and Algorithms in Support of Operational Numerical Weather Prediction", IEE Trans. Geosci. Rem. Sens., vol. 41, no. 2, Feb 2003.

[28]: Collard, A.D., "Selection of IASI channels for use in numerical weather prediction", ECMWF Technical Memorandum 532, July 2007.

[29]: "OPS-LRS User Manual", document NWPSAF-MF-UD-006, distributed with AAPP.

[30]: "AAPP Version 6 Top Level Design", document NWPSAF-MO-DS-011, distributed with AAPP.

[31]: "EPS Programme Generic Product Format Specification", document EPS-GGS-SPE-96167, available from www.eumetsat.int

[32]: "EPS/MetOp Technical Note on Orbit Prediction" Conzalo Garcia-Julian, Miguel M.Romany Merino - GMSA SA 1997

[33]: "Annex to AAPP scientific documentation: Pre-processing of ATMS and CrIS", document NWPSAF-MO-UD-027, distributed with AAPP.

[34]: "IASI Principal Components in AAPP: User Manual", document NWPSAF-MO-UD-022, distributed with AAPP.

[35]: "MAIA AVHRR Cloud Mask and Classification", L. Lavanant, 2002, available at www.meteorologie.eu.org/ici/maia/maia3.pdf

[36]: "MAIA version 4 for NPP-VIIRS and NOAA/METOP-AVHRR", Scientific User Manual, AAPP document NWPSAF-MF-UD-009, distributed with AAPP.

2.2. TERMINOLOGY

AAPP: ATOVS and AVHRR Pre-processing Package.

ADC: Analog to Digital Converter.

AIP: AMSU Information Processor.

AMSU: Advanced Microwave Sounding Unit.

ANA: Automatic Navigation Adjustment.

ARGOS: Name of the orbital bulletin emitted by CLS/ARGOS.

Ascending node (HNA) : equator satellite crossing when it comes from south pole.

ATOVS: Advanced TIROS Operational Vertical Sounder.

ATMS: Advanced Technology Microwave Sounder

AVHRR: Advanced Very High Resolution Radiometer.

Attitude: Satellite orientation according the 3 axes (yaw, roll, pitch).

Bb: black body.

Brolyd (Brouver-Lyddane): Orbit extrapolation model algorithm for TBUS bulletin.

CMS: Centre de Météorologie Spatiale (Météo-France)

CNES: Centre National d'études Spatiales.

CrIS : Cross-track Infrared Sounder

DCS: Data Collection System.

Descending node (LNA) : equator satellite crossing when it comes from north pole.

DMSP: Defense Meteorological Satellite Program

DWSS: Defense Weather Satellite System.

Earth's precession: Slow conical motion of the Earth rotation axis around a mean position corresponding to a normal direction to the ecliptic plane.

Ecliptic plane: The Earth orbital plane around the Sun.

ECMWF: European Center for Medium-Range Weather Forecasting.

Ephemeris: The list of the times of various events as: ascending and descending nodes, start and end of acquisition by a station.

EPS: EUMETSAT Polar System

FOV: Field Of View.

GAC: Global Area Coverage.

HIRS: High Resolution Infra Red Sounder.

HRPT: High Resolution Picture Transmission.

IASI: Infrared Atmospheric Sounding Interferometer.

IFOV: Instantaneous Field Of View.

IJPS: Initial Joint Polar System

Image navigation: Conversion of line and pixel numbers into latitude and longitude.

IR: InfraRed.

IWT : internal warm target

LAC: Local Area Coverage.

Mapping : for sounders = computing sounder data to another sounder grid. For imaging radiometer = imaging radiometer data segmentation to sounder ellipse.

MetOp: Meteorological Operational satellite

MHS: Microwave Humidity Sounder

MIRP: Manipulated Information Rate Processor.

MSU: Microwave Sounding Unit.

µ-waves: microwaves.

Nadir: Satellite vertical direction.

NOAA: National Oceanic and Atmospheric Administration.

NESDIS: National Environmental Satellite Data Information Service.

NORAD: North American Aerospace Defense Command

NWP SAF : Numerical Weather Prediction Satellite Application Facility.

Perigee: Satellite orbit point which is the nearest from the Earth (opposite apogee).

PM: Pulse Modulation.

POES: Polar Orbiting Environmental Satellite(s)

PRT: Platinum Resistance Thermometer.

Rg : Greenwich reference frame

Rl : local reference frame

Rs : spacecraft fixed reference frame

Rv : satellite local orbital frame

SEM: Space Environment Monitor.

SDP4: Orbit extrapolation model for deep-space object Two-Line Element sets

SGP4: Orbit extrapolation model for near-Earth object Two-Line Element sets

SSU: Stratospheric Sounding Unit.

SST: Sea Surface Temperature.

TBUS: Name of the orbital bulletin emitted by NOAA/NESDIS.

TIP: TIROS Information Processor.

TIROS: Television Infrared Observation Satellite

TOVS: TIROS Operational Vertical Sounder.

VIIRS: Visible/Infrared Imager/Radiometer Suite

VIS: Visible.

3. DESCRIPTION OF THE NOAA SATELLITES AND INSTRUMENTATION

3.1. NOAA SATELLITES

The American polar orbiting weather satellites are controlled by NOAA. The first launch occurred in 1978 with the TIROS N satellite, followed by the NOAAxx series (from NOAA6 to NOAA14), and since 1998 by the NOAA-KLM (NOAA15,16,17) and NOAA-NN' (NOAA18,19) series. Each satellite has a lifetime of nominally 4 years, though some have continued operating for very much longer than this. Two satellites must be operational at the same time. The current system records multispectral images (several spectral channels) of the Earth surface, and allows the computation of temperature and humidity profiles of the atmosphere. It is composed of two sun synchronous polar orbiting spacecraft, flying at an altitude close to 835 km. One is planned to fly in the afternoon orbit (PM), and the other in the morning orbit (AM). Due to the Earth rotation, the satellite track is translated westward with each pass. The nodal period is about 102 minutes, which means that each satellite describes 14.2 orbits per day, so the sub satellite track is not daily periodic (the same orbital configuration is achieved every 9 days). The satellite's orbital parameters drift slowly, resulting in changes in observation conditions and overpass times.

3.2. ON BOARD INSTRUMENTATION

3.2.1. Introduction

Narrow band radiometers (with channels centered on specific wavelengths) are designed to measure spectral radiances.

If the energy measured by the instrument at a given wavelength is not absorbed by the atmosphere (i.e. atmospheric window), but only by clouds, the instrument is called an imaging radiometer (e.g. AVHRR), whose purpose is to give information (reflectance or temperature) on different types of surfaces (sea, vegetation, ice, snow), or on cloud cover (top).

If the energy measured at a given wavelength is absorbed by the atmosphere, the instrument is called a sounder (e.g. TOVS/ATOVS sounding system with IR (HIRS) and microwave radiometers (MSU/AMSU/MHS)). A sounder is dedicated to measurements of the atmospheric vertical structure.

Table 1 presents the NOAAxx on board instrumentation which is covered by this documentation:

NOAA (6-14)		NOAA (15 16 and 17)		NOAA (18 and 19)	
TOVS	HIRS/2 MSU SSU	ATOVS	HIRS/3 AMSU-A AMSU-B	ATOVS	HIRS/4 AMSU-A MHS
AVHRR/2		AVHRR/3		AVHRR/3	
DCS		DCS		DCS	

Table 1: NOAAxx on board instrumentation

A short description of the previous and current instrumentation is given in the next paragraphs.

3.2.2. VIS and IR imaging radiometers

These radiometers are designed to study cloud cover and Earth surface properties. Spatial resolution depends on the instrumentation quality and the satellite height from the observation point.

AVHRR/2

is a 5 channel (0.63 to 12 µm) high resolution infrared (IR) imaging radiometer. The first two channels (0.63 and 0,86µm) measure radiance in the visible (VIS) spectral band. For example, using both channels allows the discrimination of vegetation. The three IR channels (3.74, 10.80, 12.00 µm) are generally dedicated to surface temperature determination. Using VIS and IR channels together allows determination of cloud presence and to distinguish cloud type and depth. Images from this radiometer are used for many varied applications. The internal rotating mirror scans (±55° about nadir) cross track over a swath of ±1450 km about the sub satellite track. The resolution is 1.1 km at nadir (when the observed point is at the satellite vertical) for an instantaneous field of view of 1.4 mrad. Therefore, in one day, the satellite covers twice the Earth surface, supplying one night-time and one daytime image.

AVHRR/3

has 6 channels (channel 3a: 1.61 µm, the 3.74 µm channel becomes channel 3b) in the VIS and IR spectral bands. The addition of channel 3a improves for example the discrimination between snow and clouds, and provides better aerosol detection. The resolution and the scanning characteristics remain unchanged with respect to the previous AVHRR/2 version. Only 5 channels will be received by the final user: channel 3a (day) or channel 3b (night).

3.2.3. IR and microwave sounders

The sounders have a larger spatial resolution than imaging radiometers, but they have a greater number of spectral channels. These multichannel observations allow the computation of vertical temperature and humidity profiles of the atmosphere. All but very thin cloud is opaque at IR wavelengths, so in cloudy regions microwave sounding channels, which are less sensitive to absorption by cloud, are used to retrieve atmospheric profiles.

TOVS (NOAA6-14)

is a sounding system which provides the data necessary for the retrieval of temperature and water vapour profiles. This system is composed of three different sounding units:

- **HIRS/2** is a 19 channel (from 4.3 to 15 µm) IR sounder for radiance measurements corresponding to carbon dioxide CO_2 (4.3 and 15 µm), water H_2O (6.3 µm) and ozone O_3 (9.6 µm) absorption bands. One VIS channel is dedicated to reflectance measurements (% albedo). The internal rotating mirror scans (±49.5° about nadir) a swath of ±1120 km on both sides of the sub satellite. One scan line contains 56 FOV. The resolution (pixel size on the ground) is 17.4 km at nadir for an instantaneous field of view (IFOV) of 1.25°, and 58 km at the mirror maximum deviation (largest scan angle).

- **MSU** is a 4 channel (around 50 GHz) μ-wave sounder corresponding to the oxygen O_2 absorption bands (5 mm). The internal rotating mirror scans (±47°about nadir) a swath of ±1173 km on both sides of the sub satellite track. One scan line contains 11 FOV. The resolution is 109 km at nadir and 323 km at the mirror maximum deviation (largest scan angle).
- **SSU** is a 3 channel (around 15 μm) IR spectrometer for stratospheric measurements.

ATOVS (NOAA-15-16-17 series)

is an improved TOVS version:

- **HIRS/3** is basically a modernised version of HIRS/2 with similar channel spectral characteristics. There will be only two calibration lines scan for the thermal channels.
- **AMSU-A** and **AMSU-B** replace MSU and SSU for the retrieval of temperature and water vapor vertical profiles from surface to approximately 3 hPa. **AMSU-A** is a 15 channel (around 23, 30, 50 and 89 GHz) total power μ-wave sounder. The resolution is 50 km at nadir and one scan line contains 30 FOV (rotating mirror by (+/- 48º)). **AMSU-B** is a 5 channel (around 89, 150 and 183 GHz) total power μ-wave sounder. The resolution is 17 km at nadir and one scan line contains 90 FOV.

ATOVS (NOAA-18-19 series)

- **HIRS/4** is basically a modernised version of HIRS/3 with similar channel spectral characteristics. The design changes for the HIRS/4 consist of: 1) radiant cooler operation at 95 K; 2) IFOV size reduced to 10 km; 3) inclusion of a fifth Internal Warm Target (IWT) temperature sensor; and 4) addition of a tertiary telescope temperature sensor.
- **AMSU-A** is a 15 channel (around 23, 30, 50 and 89 GHz) total power μ-waves sounder. The resolution is 50 km at nadir and one scan line contains 30 FOV (rotating mirror by (+/- 48º)).
- **MHS** is functionally similar to AMSU-B, with channels at 89, 157, 183±1, 183±3 and 190 GHz.

3.2.4. DCS

The DCS receives and retransmits data from environmental monitoring systems. It receives information as temperature, pressure, currents, wind velocity and direction from various local measurements from ground or immersed stations. Data are processed (signal demodulation, synchronization. etc.) and stored on board until the satellite can contact and transmit the collected information to a NOAA ground station. More precise characteristics are available in references [1] and [4].

3.3. DATA TRANSMISSION

Figure 1: Data transmission in HRPT format.

The radiometric and sounding data are stored on board until the satellite transmits them to a ground station. Two kinds of AVHRR data are transmitted: full resolution data LAC [1] and sampled data (mean of 4/5 pixels 1/3 line) GAC [1]. Global TIP information are also transmitted. The main acquisition stations are located near the north pole, which provide facilities for the acquisition of a great number of recorded orbits. The station transfers these data onto another satellite that can transmit the information to the main NOAA/NESDIS centre, where the data are processed and archived before distribution.

The satellite also transmits multiplexed AVHRR, TIP and AIP data, i.e. HRPT real time data, toward various line of sight acquisition stations located anywhere on the Earth surface. The frames are continuously transmitted, line by line, during approximately 15 minutes (for an orbit segment). The generated data file is about 5000 AVHRR lines (2048 pixels per line for 5 channels) representing 100 Mbytes (10 bit words) of data. The HRPT [1] data transmission is illustrated on the previous figure. Section 8.1.1 also describes the HRPT format.

The MHS instrument was designed for use on the European MetOp spacecraft. To allow it to be used on the NOAA spacecraft its data are re-formatted by the on-board MHS Interface Unit (MIU). The MIU then passes the data to the AIP, such that the MHS data occupies the same HRPT slots as are used for AMSU-B – albeit with a time delay of approximately 1 scan line. Thus from the User's point of view the processing of MHS appears similar to the processing of AMSU-B

4. DESCRIPTION OF THE METOP SATELLITES AND INSTRUMENTATION

4.1. METOP SATELLITES

The EUMETSAT Polar System (EPS) is Europe's first polar orbiting operational meteorological satellite system. The EPS consists of a series of three Meteorological Operational (MetOp) satellites, to be flown successively for more than 14 years, together with the relevant ground facilities.

The EPS is the European contribution to a joint European-US polar satellite system called the Initial Joint Polar System (IJPS). Through this international partnership, EUMETSAT will have the operational responsibility for the morning (local time) orbit with the MetOp satellites, while its US counterpart, NOAA, will cover the afternoon orbits. Data will be processed by both EUMETSAT and NOAA. The first MetOp satellite, MetOp-2 (to be called MetOp-A in operation) was launched in October 2006. Each satellite has a nominal lifetime of 5 years, with a 6 month overlap between the consecutive satellites, but in practice the lifetimes have (so far) greatly exceeded this figure.

4.2. ON BOARD INSTRUMENTATION

Under the IJPS, EUMETSAT and NOAA have agreed to provide instruments for each other's satellites. Other partners are the European Space Agency (ESA) and the Centre National d'Etudes Spaciales (CNES) of France.

The MetOp satellite carries a payload of 8 instruments for observing the planet. The AVHRR/3, HIRS/4, AMSU-A, MHS and IASI instruments are covered by this documentation.

4.2.1. VIS and IR imaging radiometers

- **AVHRR/3** is the same as on the NOAA satellites.
- The IASI sounder (see below) incorporates an integrated imager which is used to geolocate the sounder data. It is not normally used as a source of imagery for users.

4.2.2. IR and microwave sounders

- **HIRS/4, AMSU-A** and **MHS** are the same as on the NOAA satellites.
- **IASI:** The Infrared Atmospheric Sounding Interferometer represents a significant advance in the quality of the measurements injected into models for understanding and making atmospheric forecasts. The main goal of IASI is to provide atmospheric emission spectra to derive temperature and humidity profiles with high vertical resolution and accuracy. IASI is a 8461-channel interferometer. The spectral range covers 645 to 2760 wavenumbers (15.50 to 3.62 µm), with 0.25 wavenumber channel spacing. There are 30 cross-track scan positions per 8 second cycle, with 4 fields of view per scan position. The scan cycle is synchronized to that of AMSU-A. The pixel size on the ground is 12 km at nadir for an instantaneous field of view (IFOV) of 0.8225°.

4.3. DATA TRANSMISSION

There are three methods by which MetOp data are made available to users:

- Direct readout: The MetOp direct Readout Service provides to local user stations a real-time transmission of data limited to the instantaneous sub-satellite observation.
  Readout of instrument data can be achieved in the form of:
  - o Advanced High Resolution Picture Transmission (AHRPT), transmission in L-Band. It includes all instruments in full resolution. The data rate is 3.5Mbps, which is higher than that of the NOAA satellites. The formatting uses CCSDS packets.
  - o Low resolution Picture Transmission (LRPT), transmission in VHF band. It includes ATOVS in full resolution and compressed data from 3 selected AVHRR channels. The data rate is 72kbps.

- Global data via EUMETCast: The Global Data Service provides in near real-time products generated from instrument data. Data are dumped once per orbit to the Central Data Acquisition Station (CDA) (e.g. at Svalbard-Island). They are processed by the EPS Core Ground Segment at EUMETSAT, then the level 1 and level 2 products are distributed to users via EUMETCast. The delivery timeliness will be between 135 and 180 minutes after the time of measurement.

- Regional data via DBNet and EARS. The WMO coordinate a number of regional networks that acquire, process and distribute worldwide the sounder data received at AHRPT stations. This system is called the *Direct Broadcast Network* (DBNet)[1]. The EUMETSAT contribution to DBNet is called EARS (EUMETSAT Advanced Retransmission Service), and includes imager data as well as sounder data.

5. DESCRIPTION OF THE NPP AND JPSS SATELLITES AND INSTRUMENTATION

For detailed information and discussion on the scientific issues related to NPP data processing, please see document [33], which is part of the AAPP distribution.

5.1. NPP AND JPSS SATELLITES

The NPP and follow-on JPSS satellites provide NOAA's primary operational satellite in the afternoon orbit (14:00 local time northbound equator crossing), complementing MetOp in the mid-morning orbit, and the US military DMSP in the early-morning orbit.

5.2. ON BOARD INSTRUMENTATION

NPP carries a payload of 5 instruments for observing the planet. The ATMS, CrIS and VIIRS are covered by this documentation.

---

[1] http://www.wmo.int/pages/prog/sat/dbnet_en.php

5.2.1. VIS and IR imaging radiometers

The Visible/Infrared Imager/Radiometer Suite (VIIRS) is a 22-channel imaging radiometer, functionally similar to MODIS on the NASA Aqua/Terra satellites. It has three distinct groups of channels:

- Imaging: 5 channels with 370m resolution at nadir, at wavelengths of 0.64, 0.865, 1.61, 3.74 and 11.45 μm.
- Moderate: 16 channels with 740m resolution at nadir, at wavelengths of 0.412, 0.445, 0.488, 0.555, 0.746, 0.865, 1.24, 1.378, 1.61, 2.25, 3.70, 4.05, 8.55, 10.763 and 12.013 μm.
- Day-night band: 1 channel with 740m resolution across the entire swath, operating at 0.7 μm. Uses a charge-coupled device array.

5.2.2. IR sounder

The Cross-track Infrared Sounder (CrIS) is a Michelson interferometer. It has nominally 1305 channels covering the spectral bands 650-1095 cm^{-1} (713 channels, sampling 0.625 cm^{-1}), 1210-1750 cm^{-1} (433 channels, sampling 1.25 cm^{-1}) and 2155-2550 cm^{-1} (159 channels, sampling 2.5 cm^{-1}).

It samples 270 spectra per 8-second scan, with a spatial resolution at nadir of approximately 17km.

5.2.3. Microwave sounder

The Advanced Technology Microwave Sounder (ATMS) has 22 channels ranging in frequency from 23.8 GHz to 183 GHz. Functionally it is similar to the combination of AMSU and MHS, and many of the channels are identical in frequency/bandwidth to channels on AMSU/MHS. There are three new channels (51.76, 183.31±4.5 and 183.31±1.8 GHz). Spatial resolutions are as follows:

- 78km at nadir for the 23.8 and 31.4 GHz channels (5.2° beam width)
- 33 km for the 50-57 GHz sounding channels (2.2° beam width)
- 17 km for the MHS-like channels at 166 GHz and above (1.1° beam width).

There are 96 samples per 8/3 second scan line, giving a slightly wider swath than MHS.

5.3. DATA TRANSMISSION

There are three methods by which NPP data are (or will be) made available to users:

- Direct readout: The direct readout service provides to local user stations a real-time transmission of data limited to the instantaneous sub-satellite observation. NPP broadcasts at X-band only (7.8 GHz, 15 Mbps). For JPSS-1 an additional L-band downlink is planned, to contain a subset of channels/instruments.

- Global data: Global data will be made available in near-real-time by NOAA and will be re-distributed by external agencies (e.g. EUMETSAT will distribute data to European users via EUMETCast). Historical data will be available via NOAA-CLASS.

- Regional data via DBNet. Locally received data from one or more networks of X-band direct readout stations are processed at a central hub and distributed to users by mechanisms that

include the Global Telecommunications Service (GTS) and EUMETCast. Timeliness is of the order 30 minutes.

6. DESCRIPTION OF THE FY-1 AND FY-3 SATELLITES AND INSTRUMENTATION

6.1. FY-1 AND FY-3 SATELLITES

The Feng-Yun FY-1 and FY-3 satellites are the Chinese operational polar-orbiting weather satellites. They are owned by the China Meteorological Administration (CMA).

The FY-1 series started in 1988, but only FY-1D (launched in 2002) has ever been supported in AAPP. FY-1D operated until 2012.

The first in the FY-3 series, FY-3A, was launched in 2009. There is normally one satellite operating in the morning orbit and one in the afternoon orbit.

6.2. ON BOARD INSTRUMENTATION

The only instrument on FY-1D was the Multispectral Visible and Infra-red Scan Radiometer (MVISR, 10 channels).

On FY-3A, FY-3B and FY-3C, the instruments that are applicable to atmospheric sounding and imaging are as follows:

- VIRR - Multispectral Visible and Infra-red Scan Radiometer (10 channels, as on FY-1D)
- MERSI - Medium Resolution Spectral Imager
- MWTS or MWTS-2 - Microwave Temperature Sounder
- MWHS or MWHS-2 - MicroWave Humidity Sounder
- IRAS - InfraRed Atmospheric Sounder
- MWRI – MicroWave Radiation Imager

AAPP can ingest data files for MWHS, MWHS-2, MWTS, MWTS-2, IRAS and MWRI. These can be either from the ground segment for global data (operated by CMA) or from direct broadcast stations, in which case the level 1 files are generated using CMA's processing package.

6.2.1. VIS and IR imaging radiometers

AAPP does not provide any functionality for the imaging radiometers on FY-3 series, but they are described here for completeness.

The VIRR, on FY-3A, 3B and 3C is a 10-channel imaging radiometer. Channels 6-10 are similar to AVHRR channels 1-5, while channels 1-5 are additional visible channels used for ocean colour.

MERSI is a 20-channel imager, functionally similar to MODIS (on Aqua/Terra). From FY-3D, MERSI is replaced with a more advanced imager MERSI-2, with 25 channels.

6.2.2. IR sounder

The IRAS is a 26-channel visible/IR sounder. The first 20 channels are similar to HIRS, while the last 6 are for the measurement of aerosols, CO_2 and cirrus clouds.

For FY-3D onwards, IRAS is replaced by a hyperspectral IR sounder HIRAS. HIRAS is supported from AAPP v8.4.

6.2.3. Microwave sounders

The Microwave Temperature Sounder (MWTS, on FY-3A and 3B) has 4 channels, at 50.3 GHz, 53.6 GHz, 54.94 GHz, 57.29 GHz. It observes 15 earth scenes per 16-second scan. The footprint diameter is 62km at nadir (so the scene is under-sampled). The MWTS-2 (from FY-3C) is an enhanced instrument with 13 channels in the 50-55 GHz band.

The Microwave Humidity Sounder (MWHS, on FY-3A and 3B) has 5 channels in the frequency range 150-183 GHz. It observes 98 samples per scan, with a spatial resolution similar to AMSU-B/MHS. Unlike AMSU-B/MHS, it observes dual polarization at 150 GHz and has no 89 GHz channel. The MWHS-2 (from FY-3C) has 15 channels, and includes a suite of channels around the oxygen line at 118 GHz.

6.2.4. Microwave imagers

The Microwave Radiometer Imager (MWRI) is a conically-scanning microwave imager with 10 channels in the range 10.65 to 89 GHz.

6.3. DATA TRANSMISSION

FY-1D used to broadcast at L-band, using a similar format to NOAA HRPT (known as CHRPT).

The FY-3A, 3B and 3C satellites have two direct broadcast transmissions, one at L-band (1.7 GHz, 4.1 MB/s), containing the majority of the instruments, and one at X-band (7.8 GHz, 18 Mb/s), for MERSI. A software package can be obtained from CMA for generating Sensor Data Record (SDR) files from the direct broadcast streams.

For FY-3D onwards there will only be X-band, at a data rate of around 60 Mb/s.

7. AAPP PROCESSING PACKAGE DESCRIPTION

The AAPP package is intended for the ingestion and the pre-processing tasks of received HRPT data up to the retrieval of the satellite brightness temperatures. This software can be used with AVHRR, TOVS and ATOVS data.

7.1. PURPOSE AND SCOPE

For the NOAA satellites, the decommutation task performs the extraction of data particular to each instrument from the HRPT format. The data from each sounder (HIRS, MSU, AMSU, MHS) and from the imager (AVHRR) are put into separate files. The following tasks perform the computation of the calibration coefficients, the satellite navigation (satellite position calculation on its orbit) and image navigation (longitude and latitude position of the pixels, taking into account the sensor geometry, solar angles, etc.). The pre-processing tasks achieve the conversion of the raw HRPT data (Earth and atmosphere VIS and IR radiances) into physical parameters (brightness temperatures, albedo) and

perform data mapping between the measurement grids of the different instruments (AVHRR/HIRS, AMSU-MHS/HIRS mapping...).

In the case of MetOp, it is the responsibility of the ground station to convert received AHRPT data to "PFS level 0 format". In this format the data streams for the various instruments are already separated. Thus there is no MetOp decommutation task. Instead, tools are provided within AAPP to convert PFS level 0 files to AAPP level 1a format – for AMSU-A, MHS, HIRS and AVHRR. The level 1a files can then be processed by the core AAPP calibration and pre-processing modules.

For IASI, processing to level 1c may, if required, be performed by OPS-LRS (Operational Software – Local Reception Station) package. A technical description of this package, together with references to scientific documentation, is given in the OPS-LRS User Manual [29].

In the case of NPP and JPSS, it is the responsibility of the ground station to convert received X-band direct broadcast data to "Sensor Data Record" format. An external software package is required for this task. At the time of writing, two packages are being advertised to do this task:

1. The *International Polar Orbiter Processing Package* (IPOPP) developed by the NASA Direct Readout Laboratory.

2. The *Community Satellite Processing Package* (CSPP) produced by the University of Wisconsin, with the heritage of the *International MODIS/AIRS Processing Package* (IMAPP).

Both of the above packages are based on the *Algorithm Development Library* (ADL) which is a Linux port by Raytheon of the operational NOAA ground segment software (called IDPS - *Interface Data Processing Segment*).

AAPP may also be used to process global or regional NOAA, MetOp or NPP data received elsewhere, for example:

- AMSU, HIRS and MHS level 1b data from the NOAA archives

- Global MetOp data received from EUMETSAT (e.g. via EUMETCast). AAPP includes the necessary BUFR decoding and encoding routines

- Global NPP data in BUFR format received from NOAA or from EUMETSAT

- Global NPP data in HDF5 Sensor Data Record format from CLASS.

7.2. GENERAL DESCRIPTION

AAPP version 8 presents three distinct components, as was the case for AAPP versions 6 and 7:

- The core AAPP task, including NPP-specific routines

- Tools to interface the core AAPP with the specific formats of MetOp data.

- A suite for processing IASI data to level 1c, based on the CNES-supplied IASI OPS (Operational Processor Software), named OPS-LRS for Local Reception Station..

The core AAPP can be broken down to six major tasks:

1. Decommutation (only useful for direct acquisition of NOAA data)

2. Calibration/satellite navigation/localisation

3. Preprocessing step 1 (atovin): Apply calibration coefficients, convert radiances to brightness temperatures.

4. Preprocessing step 2 (atovpp): Instrument mapping on another instrument grid

5. AVHRR mapping on HIRS and cloudmask (avh2hirs)

6. Tools to perform a range of tasks, including BUFR encode/decode, reading of HDF5 files, etc.

The following figures (Figure 2, Figure 3, Figure 4, Figure 5) show the different processing chains according to the origin of the data. The figures don't make mention of pre-NOAA-K satellites, for which the MSU instrument was used instead of AMSU-A and AMSU-B/MHS.

The different levels of AAPP data are defined as follows:

level0: raw HRPT data.

level1a: separated data for each instrument.

level1b: geo-referenced and calibrated data (reversible: calibration coefficients are separated from raw data).

level1c: geo-referenced and calibrated temperatures and albedo (non-reversible: calibration coefficients are applied to numerical data). In the case of IASI, level 1c implies Gaussian apodisation.

level1d: mapped and filtered data (cloud mask).

Note that NOAA use the following product naming convention for NPP/JPSS data:

raw data records (RDR): raw data, separated for each instrument.

temperature data records (TDR): calibrated antenna temperatures (only applicable to microwave sounder).

sensor data records (SDR): calibrated brightness temperatures

environmental data records (EDR): retrieved quantities

climate data records (CDR): A subset of EDRs, with traceability suitable for climate studies.

Figure 2: AAPP processing chain for NOAA satellites.

*: AMSU-B l1c and AMSU-B l1d contains MHS data for NOAA-18.

The script, named **AAPP_RUN_NOAA**, allows the user to link up the different independent tasks (see Installation Guide).

Figure 3: AAPP processing chain for MetOp satellites.

*: MHS l1c and MHS l1c data are ranged into files named AMSU-B l1c and AMSU-B l1d.

Figure 4: AAPP processing chain for NOAA -1b archive data.

(*): A tool to partially convert AVHRR NOAA l1b into AVHRR AAPP l1b is provided in AAPP (hrpt1b_noaa.exe). See the format documentation for the differences between the two formats.

Figure 5: AAPP processing chain for MetOp data received via EUMETCast.

NPP processing
In the case of NPP, AAPP contains the ability to pre-process the ATMS and CrIS sounder data, plus a VIIRS cloud mask and the ability to map VIIRS to CrIS. ATMS and CrIS pre-processing is discussed in detail in [33]. The NPP processing chain within AAPP comprises the following elements:

1. Transform SDR files from BUFR or HDF5 to internal AAPP format

2. Modify the AAPP effective beam width (to reduce noise and/or match footprints for different channels)

3. Run atovpp in order to:
   - map ATMS to CrIS
   - generate derived ATMS cloud quantities

- perform spectral and/or spatial thinning for CrIS

4. Optionally, BUFR encode the outputs.

7.3. <u>AAPP MODULES</u>

The tasks are separated for TOVS/ATOVS and AVHRR. The main modules are:

7.3.1. <u>Ingest:</u>

Decommutation (NOAA satellites only):

DECOMMUTATION performs the interface between acquisition and processing system. This function is specific to the AAPP installation site and can be modified by the user if the acquisition system doesn't respect HRPT format. This module calls **HRPTDC** to perform decommutation task.

HRPTDC (**ATOVDC** and **AVHRDC**) performs the decommutation task: It reads the raw (level 0) HRPT data streams and puts data from the sounding instruments (HIRS, AMSU-A, AMSU-B, MHS, MSU) and from the AVHRR radiometer into separate files (level 1a).

MetOp tools:

The format conversion tools for MetOp allow the conversion of PFS level 0 format (from the reception station) to AAPP level 1a format – for AMSU-A, MHS, HIRS and AVHRR. Each instrument uses a separate conversion program.

There is also a tool *aapp-eps_avhrrl1b* to convert AVHRR AAPP level 1b format to PFS level 1a, for use with OPS-LRS, and a tool *convert_iasi1c* to convert IASI level 1c PFS format (from OPS-LRS) to an AAPP format that can be ingested by ATOVPP.

The tool *convert_avh1b* can be used to convert AVHRR PFS level 1b to a "pseudo"-AAPP level 1b format. In this format, the "counts" are not instrument counts, they are actually scaled radiances, with the "calibration coefficients" (slope and offset to apply to the "counts") being set to constant values.

Satellite and image navigation - Calibration coefficients:

ATOVCL(=HIRSCL,AMSUACL,AMSUBCL,MHSCL,MSUCL) performs the satellite navigation, the Earth localisation of the pixels, and the calibration coefficients calculation for each TOVS/ATOVS instrument.

AVHRCL performs the same tasks for the AVHRR radiometer.

At the end of this procedure, separated files of Earth located data and calibration coefficients exist. Those (level 1b) files are archived.

7.3.2. <u>Pre-processing:</u>

Calibration:

ATOVIN applies the calibration coefficients calculated by **ATOVCL** to the numeric counts for radiance conversion. Before that, for AMSU-A data, a moon detection/correction is done. For AMSU-B data, corrections are applied. Then **ATOVIN** converts each channel radiance into brightness temperature for each TOVS/ATOVS instrument.

At the end of this procedure, separate files of Earth located brightness temperature data exist. Those (level 1c) files are archived.

Mapping:

ATOVPP recognises data contaminated by precipitation and maps data between the measurement grids of the different instruments (for examples: HIRS + AMSU-A + AMSU-B/MHS on HIRS grid, HIRS+MSU on HIRS grid, AMSU-A + AMSU-B on AMSU-B grid, AMSU-A + MHS on IASI grid).

The standard '**AAPP_RUN_NOAA**' implements any of these mappings, controlled via the "-i" and "-g" options.

Mapping - Cloud mask:

AVH2HIRS applies the calibration coefficients (calculated by **AVHRCL**) to AVHRR counts and converts radiance into brightness temperatures, maps AVHRR data to the HIRS FOV, and optionally makes the cloud mask (**MAIA4,** for AAPP version 8 and later) in the HIRS ellipse for contaminated pixels discrimination. At the end of this procedure, a level 1d file exists (HIRS level 1d).

The **MAIA4** cloud mask can also be generated on the AVHRR grid.

7.3.3. IASI ingest and pre-processing

The IASI ingest and calibration task is done by the **OPS-LRS** software. It processes IASI instrument data from PFS level 0 (raw instrument data) through to PFS level 1c that includes calibrated, geolocated, Gaussian-apodised radiances.

The software is based on the software used in the EPS Core Ground Segment that was supplied to EUMETSAT by CNES. It has been modified by the NWP SAF for portability and to allow distribution with AAPP.

IASI level 1c data can be ingested by ATOVPP, which can perform various pre-processing operations, depending on the user options that are specified:

- map AMSU/MHS to IASI
- channel selection
- Principal Components (PC) analysis

These are discussed more fully in the following sections. PC processing is also discussed in [34]. The output of this step is an IASI Level 1d file.

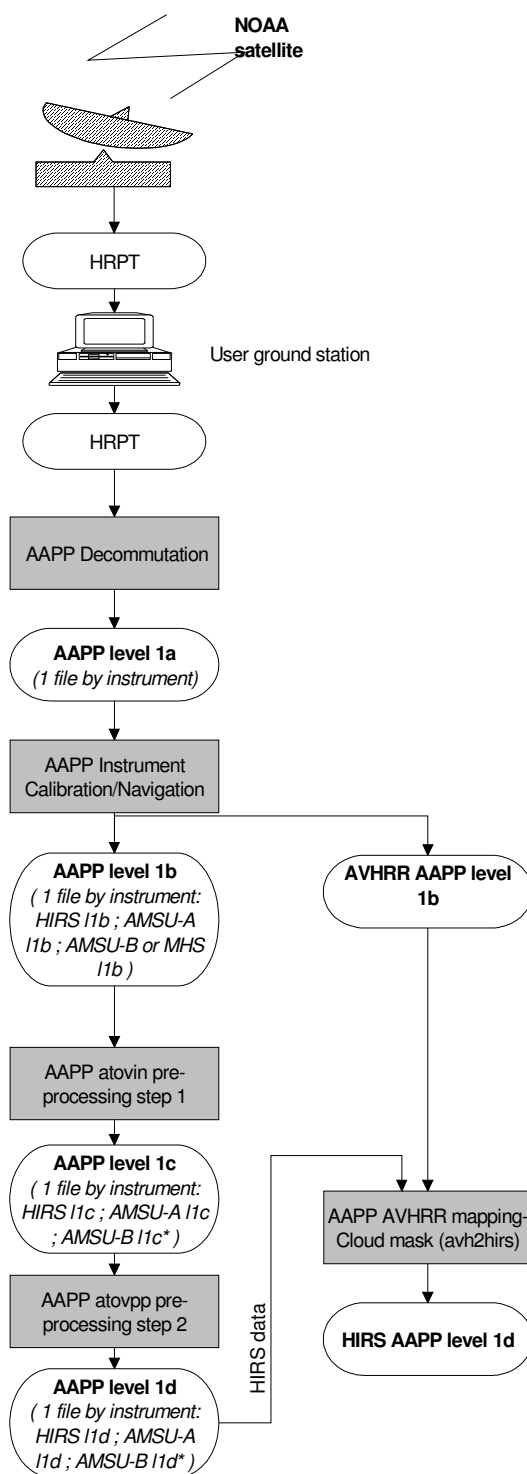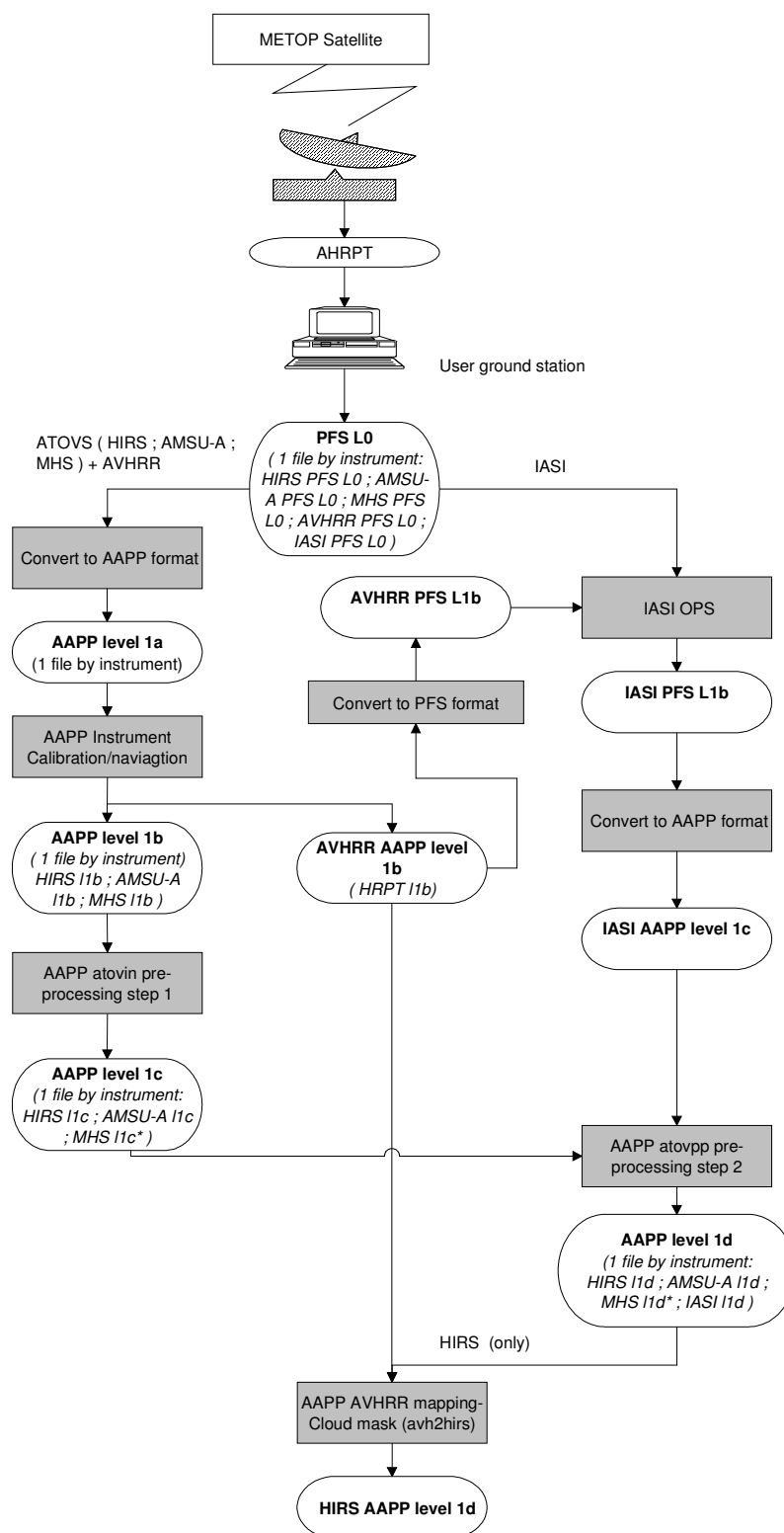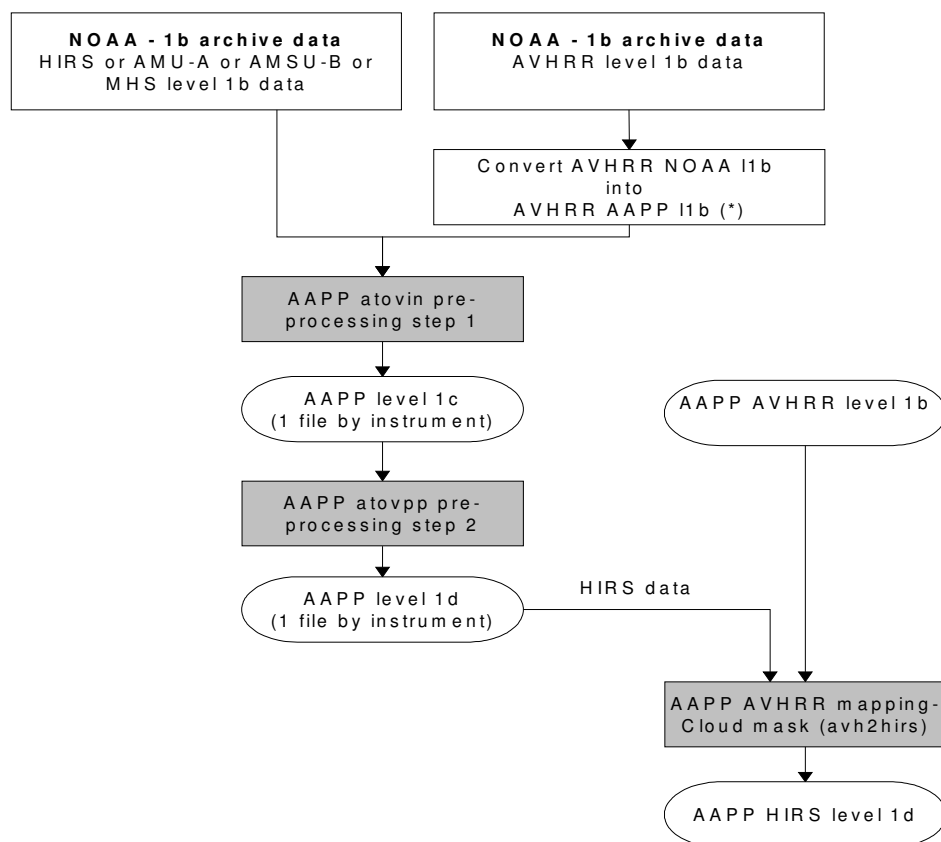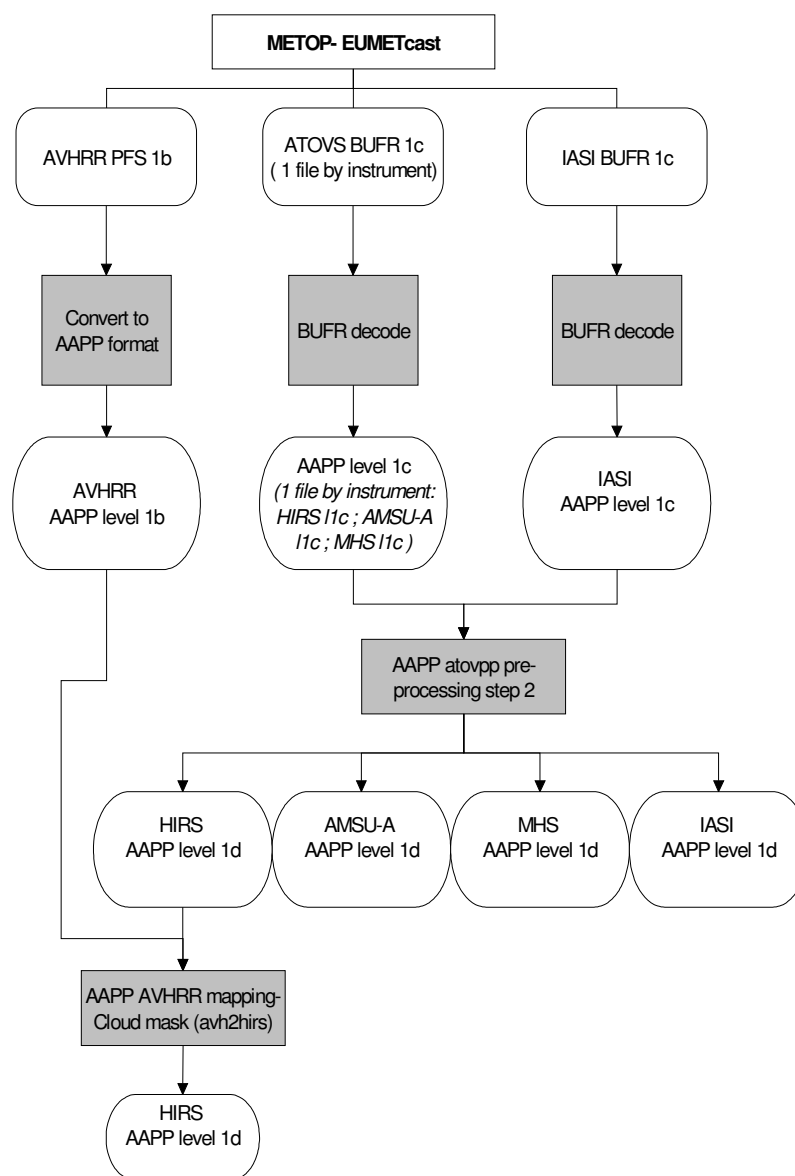| NWP SAF	AAPP DOCUMENTATION SCIENTIFIC DESCRIPTION	Doc ID : NWPSAF-MF-UD-001 Version : 8.1 Date : October 2019

8. AAPP SCIENTIFIC DESCRIPTION

This part will not mention the description of the OPS-LRS software. The scientific documents related to IASI are available from the AAPP "supplementary downloads" section of the NWPSAF web site: follow the link to "OPS-LRS auxiliary data" and then "reference_docs". The tar file includes the documents IA-SB-2100-9462_0503 "Spécification Technique de Besoin du logiciel opérationnel IASI" and IA-DF-0000-2006-CNE "Dossier de définition des algorithmes IASI". They are in French.

8.1. DECOMMUTATION

This section is applicable to the NOAA satellites only.

HRPT (High Resolution Picture Transmission) is a real time transmission of full resolution images coming from the different instruments on board the NOAA satellites. The AVHRR, TIP (HIRS, MSU, DCS, housekeeping data...), and AMSU/MHS data are multiplexed, which means that one HRPT data stream contains mixed information related to all instruments. Data are organized into major and minor frames, in order to easily extract the information belonging to each instrument.

The scope of the decommutation task is to recognize and to extract, from the HRPT format, the measurements and the telemetry data of each instrument. It results in the creation of a separate file of raw data for each instrument.

8.1.1. HRPT format general description

Description

The format of the HRPT, TIP and AIP minor frames is assumed to be as defined in the NOAA referenced document [1]. It is advised to refer to these documents for a precise definition.

The HRPT major frame is made of 3 minor frames. Since the AMSU sounder has appeared on NOAA-K series (and so MSU and SSU have disappeared), the frame structure has changed. Table 2 and Table 3 show one HRPT major frame for both cases.

n°1	synchro + id + date	telemetry + calibration	5 TIP cycles (n)	spare	AVHRR video (n)	aux. synchro
n°2	synchro + id + date	telemetry + calibration	5 TIP cycles (n)	spare	AVHRR video (n+1)	aux. synchro
n°3	synchro + id + date	telemetry + calibration	5 TIP cycles (n)	spare	AVHRR video (n+2)	aux. synchro
words	12	91	5x104	127	10240	100

Table 2: One HRPT major frame and its 3 minor frames for pre-NOAA-K satellites.

n°1	synchro + id + date	telemetry + calibration	5 TIP cycles (n)	spare	AVHRR video (n)	aux. synchro
n°2	synchro + id + date	telemetry + calibration	backfill	spare	AVHRR video (n+1)	aux. synchro
n°3	synchro + id + date	telemetry + calibration	5 AIP cycles (n)	spare	AVHRR video (n+2)	aux. synchro
words	12	91	5x104	127	10240	100

Table 3: One HRPT major frame and its 3 minor frames for NOAA-K series.

Each minor frame is a record of 11090 words length. The input minor frames are assumed to be 10 bit words unpacked into the least significant bits of 16 bit words. The exact format of the HRPT minor frame depends on the hardware of the reception station, which means that the frames have to be read by centre specific routines. The HRPT minor frames are numbered here from 1 to 3. Each minor frame contains one different AVHRR line (eg. from line n to n+2 for this major frame), whereas the TIP data (of 5 TIP cycles) are repeated 3 times in the same major frame (eg. 3 times line n) for pre-NOAA-K satellites. For NOAA-K and N series, the first minor frame contains 5 TIP cycles data, the second minor frame contains backfill data, and the third minor frame contains 5 AIP cycles data.

HRPT minor frame format:

- Number of minor frames per second: 6.
- Size: 11090 words distributed in:
  - frame synchronization: 6 words.
  - identification: 2 words (synchro. type, cycle number, satellite number, resynchro., AVHRR 3a/3b channel).
  - time code: 4 words.
  - telemetry: 10 words (AVHRR calibration ramp, PRT numeric counts...).
  - AVHRR calibration warm target view data or back scan data: 30 words.
  - AVHRR space numerical counts: 50 words.
  - synchronization: 1 word.
  - 5 TIP/TIP/TIP cycles or TIP/backfill/AIP: 5x104 words (Earth observations).
  - spare words: 127 words.
  - AVHRR video: 10240 words (Earth observations).
  - auxiliary synchronization: 100 words.

80 AIP minor frames are required to give 1 AMSU-A and 3 AMSU-B/MHS scan lines. 64 TIP minor frames are required for 1 HIRS scan line. 256 TIP minor frames are required for 1 MSU scan line, and 320 consecutive TIP minor frames correspond to one TIP major frame (of 32 seconds).

TIP minor frame description (NOAA-K and N series):

One TIP minor frame contains HIRS, DCS, SEM, and SBUV (Solar Backscatter Ultra violet Spectral Radiometer for near ultraviolet solar and terrestrial radiation measurements) data for the NOAA-K series (HIRS, MSU, SSU, DCS, SEM and SBUV for the previous satellites), but also the housekeeping parameters which are required for the data navigation or calibration pre-processing. DCS, SEM and SBUV data can also be extracted from the HRPT format, but are not used by the AAPP operational scheme.

- One TIP minor frame: each 100 ms.

- Size: 103 words (here 1 word is in fact 1 byte) distributed as follows:
  - frame synchronization: 3 words (0, 1, 2).
  - status: bits 1 to 6 of word 3 (mode: 'orbital', 'memory dump', 'dwell', 'boost', major frame counter incremented each 320 minor frames).
  - 'dwell' mode address: bits 7 to 8 of word 3 and bits 1 to 7 of word 4 (9 bits dwell mode address (between 0 and 511) of analog channel that is being monitored continuously).
  - 9 bits minor frame counter: bit 8 of word 4 and word 5 (from 0 to 319).
  - command verification: 2 words (bits 9 to 24 of each valid received command are placed in the 16 bit slots of telemetry words 6 and 7).
  - time code: 5 words (8 to 12) only given in minor frame 0.
  - Digital 'B'-1 telemetry: 1 word (8). There are 256 digital B-1 inputs. Each input has its own channel number between 0 and 255. A subcommutation system allows selection of each input once every 3.2 s.
  - Analog-1 32 s telemetry: 1 word (9). This format is 320 words length that repeats every 32 s. Each input has its own analog channel number. 191 channels are sampled once every 32 s, and twice for the 64 other channels.
  - Analog-1 16 s telemetry: 1 word (10). This format is 160 length. Each input has its own analog channel number. 128 channels are sampled once every 16 s.
  - Analog-1 1 s telemetry: 1 word (11). 10 channels are sampled once per second.
  - Digital 'B'-2 telemetry: 1 word (12). There are 256 digital B-2 inputs. Each input has its own channel number between 0 and 255. A subcommutation system, allows selection of each input once every 3.2 s.
  - Analog-2 16 s telemetry: 1 word (13). This format is 160 length. Each input has its own analog channel number. 128 channels are sampled once every 16 s.
  - DAU-1: 1 word (14). 8 bit housekeeping telemetry words are formed and read out at the rate of 10 words/s.
  - DAU-2: 1 word (15). 8 bit housekeeping telemetry words are formed and read out at the rate of 10 words/s.
  - HIRS/3 or 4 numeric counts: 36 words between 16 and 93. rate: 360 words/s.
  - SEM numeric counts: 2 words (20 and 21). rate: 20 words/s.
  - DCS numeric counts: 32 words between 18 and 95. rate: 320 words/s.
  - SBUV numeric counts: 4 words (36, 37, 80, 81). rate: 40 words/s.
  - CPU telemetry: 12 words (46 to 51 and 96 to 101). Bus A and B CPU data bus.
  - CPU data status: 2 bits of word 103. Data received or incomplete.
  - parity: bit 3 to 8 of word 103.

There are 7 different telemetry groups. Their respective position in the format depends on the selected TIP mode (the mode described here is 'orbital'). These digital and analog channels provide the required signals (synchronization and clock signals, power...) for all the on board electronics (processors, converters, drivers, memories, instruments, motors...), but also provide data links between the different interfaces (data bus...).

AIP minor frame description (NOAA-K series):

The spacecraft's AMSU Instrument Processor (AIP) collects digital data from the AMSU-A and AMSU-B sensors. These data consist of earth view pixel data, housekeeping data and space and blackbody view data.

- Size: 103 words distributed:
  - frame synchronization: 3 words.

- spare: 1 word.
- minor frame counter: 1 word (from 0 to 79).
- major frame counter: 1 word (incremented every 80 minor frames, overflow to 0 synchronous with the TIP 32 s major frame pulse).
- spare: 2 words.
- AMSU-A1 numerical counts: 26 words (AIP read out at the rate of 260 words/s).
- AMSU-A2 numerical counts: 14 words (AIP read out at the rate of 140 words/s).
- AMSU-B numerical counts: 50 words (AIP read out at the rate of 500 words/s).
- spare: 4 words.
- AMSU parity: 1 word.

AIP minor frame description (NOAA-N series):

The spacecraft's AMSU Instrument Processor (AIP) collects digital data from the AMSU-A and MHS/MIU (MHS Interface Unit) sensors. These data consist of earth view pixel data, housekeeping data and space and blackbody view data.

- Size: 103 words distributed:
  - frame synchronization: 3 words.
  - spare: 1 word.
  - minor frame counter: 1 word (from 0 to 79).
  - 8 second frame counter: 1 word (last two bits are major (8-sec) frame counter. It is incremented every 80 minor frames, bits 7 and 8 of minor frame 5 will count 8-second intervals, the count overflowing to 0 synchronous with the TIP 32-second major frame pulse).
  - MIU/MHS Status: 2 words (8-bit words formed by the MIU to record status of the MHS and the MIU and read by the AMSU Information Processor at an average rate of 20 words per second).
  - AMSU-A1 numerical counts: 26 words (8-bit words are formed by the AMSU-A1 experiment and are read out by the AMSU Information Processor (AIP) at an average rate of 260 words per second).
  - AMSU-A2 numerical counts: 14 words (8-bit words are formed by the AMSU-A2 experiment and are read out by the AIP at an average rate of 140 words per second).
  - MHS numerical counts: 50 words (8-bit words are formed by the MHS experiment and are read out by the AIP through the MHS Interface Unit at an average rate of 540 words per second).
  - spare: 4 words.
  - bit TIP Parity (AMSU): 1 word.

8.1.2. level1b format general description

Description :

A detailed file format description stemming from the decommutation process is given in the AAPP data format document. The NOAA distributes level1b format data. The idea that is followed here is to keep the same file structure for 1a (after decommutation step) and 1b (after navigation and calibration steps) levels. The difference between 1a and 1b data is that some housekeeping data are converted in 1b and not in 1a, some calibration and navigation indicators are flagged in 1b, the fields relative to navigation (orbital parameters, angles, positions, velocities, attitude...), and calibration (coefficients...) are filled up.

Some general principles were adopted for the format elaboration:

- The file header can be composed of several records. The header records length is the same as for the data records for a given instrument. Fillers are provided to keep record lengths multiples of 512 bytes.
- All character fields are ASCII and all fields are aligned.
- The dates are corrected from clock errors, and the day is Julian (reference 01/01/1950).
- Data are unpacked into 16 bit words.
- Real type data are converted to integer by a 10 power multiplication.

1b header general structure:

- **General information:** format version, satellite identification, data type, start and end dates, calibration parameter identification.
- **Data set quality indicators:** instrument status, number of lines or records, missing lines, parity errors, clock status, Earth location errors, PACS status bit field, data source.
- **Calibration parameters:** ramp non linearity for each spectral channel, calibration algorithm identification, mean coefficients and standard deviation.
- **Albedo and temperature-radiance conversion parameters:** central wave numbers, correction and non-linearity coefficients...
- **Navigation parameters:** navigation status, 3 attitude angles, orbit date, 6 orbital parameters, position-velocity vectors, Earth/Sun distance ratio.
- **Analog and digital telemetry conversion coefficients:** coefficients for PRT numerical counts to resistance or temperature conversion, numeric counts to current or voltage conversion...
- Filler.

1b record scan line general structure:

- **Scan line information:** date, line number, navigation and calibration quality indicators.
- Quality indicators
- Calibration coefficients.
- **Navigation data:** TIP attitude angles, zenith and azimuth angles in the satellite and sun directions, relative azimuth angles, latitudes/longitudes...
- **Instrumental measurements:** Earth view numeric counts for all spectral channels and all line FOV.
- Digital and analog housekeeping telemetry data:
- Filler.

8.1.3. Ingest format for MetOp data

AAPP/MetOp accepts MetOp data encoded in PFS level 0 format for pre-processing. This format is described in EPS-GGS-SPE-96167 [31].

It is the responsibility of the user to produce correct PFS L0 from the CCSDS instrument packets. Each instrument data shall be encoded in a separate file, with packets sorted by time.

After the decommutation stage traditional AAPP 1B format is used.

8.2. NAVIGATION

8.2.1. Definitions

This section presents the definitions of the main parameters used in the navigation function. More details can be found in [17], [18] or directly in the Fortran code comments. The sign conventions of most parameters (and the reference frame axis positive directions) are somewhat arbitrary; the ones mentioned here are those used in AAPP.

The navigation is the conversion of the image coordinates, line and pixel numbers, into geographical coordinates, latitude and longitude, and reciprocally. The sun and satellite zenith azimuth angles are also calculated.

The Earth's surface is approximated by an ellipsoid whose center is at the Earth's gravity center.

Greenwich terrestrial reference frame
- The centre is at the Earth's gravity centre.
- The x-axis is the line from the Earth's gravity centre to the intersection between the equator and the Greenwich meridian, which defines the positive direction.
- The y-axis in the equatorial plane, normal to the x- and z-axis.
- The z-axis is the polar axis, positive toward the North Pole.

This Earth-fixed reference is widely used is AAPP. Using the Earth's ellipsoid parameters, the Cartesian coordinates in this frame can be converted in latitude, longitude, altitude, and reciprocally.

Local (geographical) vertical of a point: normal to the Earth's ellipsoid that contains the point, positive upward (the point may be on the Earth' surface or not).

(Geographic) latitude of a point: angle between the equatorial plane and the local vertical of the point, positive toward north.

Beware that the geographic latitude is not equal to the geocentric latitude, which is the angle between the equatorial plane and the line connecting the Earth' center and the point.

(Geographic) longitude : angle between the Greenwich meridian and the meridian of the point, positive toward east.

The navigation function calculates the zenith and azimuth angles of the sun or satellite, seen from an observation point, which is generally the viewed pixel and, for tracking calculations, the ground station. A local reference frame relative to the observation point is introduced for that purpose.

Local reference frame of an observation point
- The center is at the observation point.
- The x-axis is in the horizontal plane and the half plane that contains the meridian of the point, positive toward south.

- The y-axis is in the horizontal plane, normal to the x- and z-axis.
- The z-axis is the local vertical of the observation point.

The horizontal plane is defined as normal to the local vertical, a vertical plan is any plane that contains the local vertical.

For an object, sun or satellite, seen from an observation point:

- The **zenith angle** is the angle between the local vertical and the point-to-object vector, it varies from 0 to 180 degrees.
- The **azimuth angle** is the angle between a vertical half plane containing the north direction (i.e. opposite to the local reference frame x-axis) and the point-to-object vector ; this angle varies from –180 to 180 degrees, is 0 at true north and positive toward east.

The azimuth angle definition is that of the NOAA level 1b. Beware that the sign conventions of the azimuth angle and local reference frame x-axis are not natural.
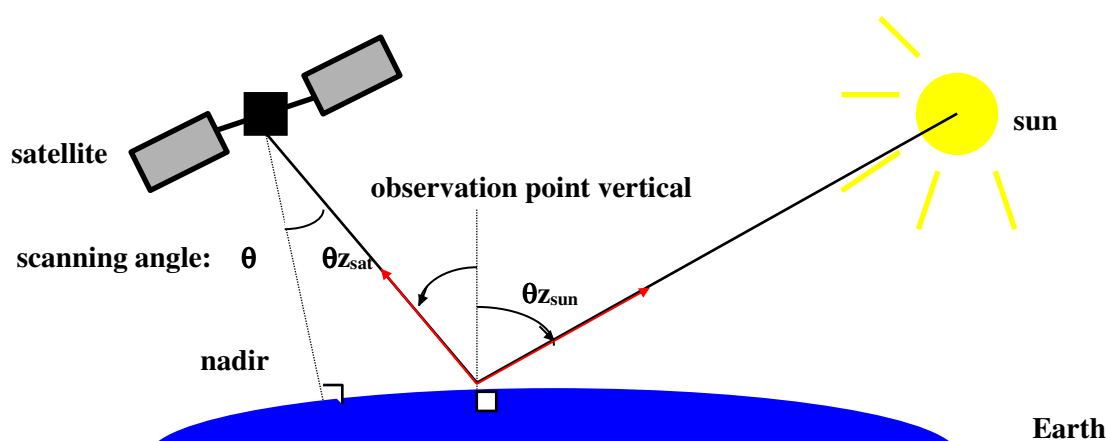
Figure 6: Sun and satellite zenith angles

The sun and satellite zenith angles are generally not in the same plane. The satellite zenith angle and the radiometer scanning angle are in slightly different planes.
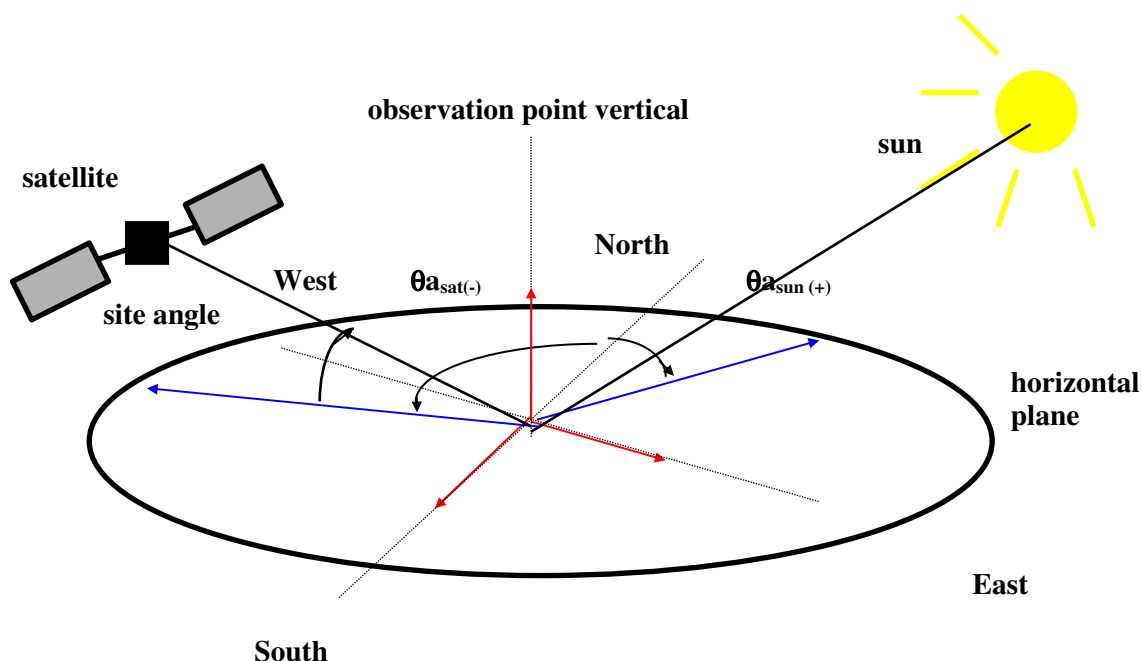
Figure 7: Sun and satellite azimuth angles

Spacecraft nominal orientation reference frame

This frame has a rather complicate definition based on the satellite velocity and local vertical, which depends on the satellite attitude mode.

"Local normal pointing mode"
- The center is at the satellite gravity center.
- The x-axis is opposite to the local terrestrial vertical (positive toward the Earth).
- The y-axis is normal to the x- and z-axis (nearly collinear to velocity, opposite in direction).
- The z-axis is normal to x-axis and to the satellite velocity, positive in the direction of the angular momentum vector of the orbit (nearly orthogonal to the orbit plane).

The local normal pointing mode is the usual mode of NOAA POES:

"Yaw steering mode"

The definition is the same as for the NOAA POES operational mode except that the z-axis is normal to x-axis and to the satellite velocity relative to the Earth.

The yaw steering mode is the usual mode of MetOp.

"Geocentric mode"
- The center is at the satellite gravity center.
- The x-axis is directed from the satellite to the Earth center.
- The y-axis is normal to the x- and z-axis (nearly collinear to velocity, opposite in direction).

- The z-axis is normal to x-axis and to the satellite velocity, positive in the direction of the angular momentum vector of the orbit, it is orthogonal to the orbit plane.

The geocentric mode is not a usual mode of NOAA POES neither of MetOp.

Spacecraft-fixed reference frame

- The center is at the satellite gravity center.
- The x-axis is the "vertical" axis of the spacecraft.
- The y-axis is the "longitudinal" axis of the spacecraft.
- The z-axis is the "transversal" axis of the spacecraft.

These axes are defined precisely with respect to some elements of the spacecraft structure, their positive direction being consistent with the spacecraft nominal orientation.

The spacecraft-fixed reference frame should be perfectly aligned with the spacecraft nominal orientation reference frame, but it differs from it by three small rotation angles: yaw about the x-axis, roll about the y-axis and pitch about the z-axis. The sign conventions are the following:

yaw > 0   : the spacecraft longitudinal axis is orientated toward the right of the trajectory
roll > 0   : the spacecraft vertical axis is on the right of the sub-track
pitch > 0   : the spacecraft vertical axis is behind the sub-point

So, the satellite "**attitude error**" or "attitude" represents an orientation error of the spacecraft with respect to its nominal value. It is expressed by three small **attitude angles**, the **yaw, roll and pitch**.

Instrument-fixed reference frame

- The center is at the satellite gravity center.
- The x-axis is nearly aligned with the "vertical" axis of the spacecraft.
- The y-axis is nearly aligned with the "longitudinal" axis of the spacecraft.
- The z-axis is nearly aligned with the "transversal" axis of the spacecraft.

These axes are defined precisely with respect to some elements of the instrument structure. They should be perfectly aligned with the spacecraft-fixed axes, but differ from them by three small rotation angles: in yaw about the x-axis, in roll about the y-axis and in pitch about the z-axis. These **misalignment angles** are constant during the satellite lifetime.

Scanning plane: many instruments considered in AAPP (AVHRR, HIRS, AMSU) are cross-track scanning radiometers, i.e. having a scanning plane normal to the spacecraft longitudinal axis. AAPP may also handle an instrument with a tilted scanning plane, which corresponds to an additional rotation about the spacecraft transversal axis..

Conical scanning: the radiometer viewing direction lies in a cone and rotates about the cone axis at a constant speed, the cone axis being in the instrument longitudinal plane, aligned with the vertical axis or inclined forward or backward.

8.2.2. Principles of the navigation method

The AAPP navigation method is based on precise geometrical calculations using time varying parameters: satellite position and velocity, satellite clock error and satellite attitude (or orientation) and constant parameters defining the scanning of each instrument (AVHRR, HIRS, AMSU or MHS). It

has been designed initially for NOAA POES data and generalized in order to process MetOp data or, possibly, other satellite data. This section summarizes the essential features of the method, without presenting the equations. The main equations together with a detailed description of the method are presented in [17], some additional equations can be found in [18] and the equations corresponding to AAPP-5 and 6 are given in [22].

The satellite position and velocity are calculated by an analytical orbit extrapolation model that ingests daily orbital elements of the satellite. For NOAA satellites, two options are proposed, based on TBUS bulletins or Two-Line Element sets. For MetOp satellites, two options are also proposed based on Two-Line Element sets or SPOT-5 element sets.

While the orbit prediction and all navigation calculations are made in Universal Time (UT), the NOAA image data are dated with the satellite clock, which drifts and is periodically reset. Until 2002, the satellite clock error values issued by NOAA/NESDIS in the TBUS bulletin were used to correct the satellite clock times into UT values but this step is no longer required.

The scanning direction (from the satellite to the viewed pixel) is defined in a spacecraft instrument-fixed reference frame, which slightly differs from its nominal orientation due to the misalignment angles. These errors are taken into account in the geometrical calculations, assuming constant misalignment angles and a constant value attitude error over a whole HRPT acquisition. The attitude error is expected to vary from one pass to another.

The various steps of the method are clearly separated. The satellite orbit prediction produces an intermediate file of position and velocity vector, which allows replacing the orbit extrapolation program without changing the other navigation modules. Correcting for the satellite clock error can be by-passed. The actual values of the satellite attitude, if any, are read in a separate file.

For NOAA POES, estimating the actual satellite attitude is not straightforward since NOAA/NESDIS does not distribute this information to the users. The AAPP user has several options to cope with this problem:

- use the default value of each satellite, which is included in AAPP Fortran code; this option only eliminates the systematic errors, which have been well established on historical data,
- calculate some landmark navigation errors and derive from them the attitude error, through some of the AAPP routines,
- interface AAPP with the add-on software ANA-3 (enquiries about ANA should be directed to Météo-France).

8.2.3. Satellite position and velocity

Orbit prediction

The satellite position and velocity can be calculated by a complex and precise numerical model ingesting numerous trajectory measurements or by a simple analytical model ingesting a set of orbital elements (position-velocity or elliptical parameters), which is valid at a given date. Several services NOAA/NESDIS, NASA NORAD, CNES and Eumetsat routinely produce bulletins containing orbital

elements of the NOAA/MetOp satellites, which have been derived from precise orbit calculations. The user can enter these orbital elements into a simple analytical orbit prediction model to compute the satellite position and velocity at any time. Better results are expected if the analytical model is consistent with the previous orbit calculations. NOAA/NESDIS, which distributes orbital elements in the TBUS bulletin, recommends and distributes an orbit extrapolation model, called **BROLYD**. NORAD distribute the Two-Line Element sets and the orbit extrapolation models **SGP4** (for near-Earth satellites having a period lower than 225 minutes) and **SDP4** (for deep-space satellites). These orbit extrapolation models have been implemented in the AAPP package without any change. EUMETSAT have in the past distributed the **SPOT-5** element sets and the orbit extrapolation model **SPM** [31], but these are no longer used.

Orbital element ingest

The orbital elements are not directly used for navigations calculations, but after an "ingest" step, which decodes the TBUS bulletin or the Two-Line Element file and controls the quality of newly received sets of orbital elements. This control uses the BROLYD, SGP4 or SDP4 model to calculate a forward extrapolation error of the last preceding valid set onto the current set and a backward extrapolation of the current set onto the preceding one. If these are lower than a threshold, the current set is considered as valid. This control eliminates a few orbital element sets having a poor quality when compared to the others. All received bulletins are stored and some essential information (epoch time, orbit, quality...) is stored in an historical index file. The ingest step allows the addition of old sets of orbital elements.

Position and velocity calculation

The satellite position-velocity is required at any step of the navigation and some equations are solved by iteration. Using the orbit extrapolation model whenever position-velocity value is needed is not realistic. Therefore, a two-step method is used:

- The extrapolation model produces position and velocity vectors every two minutes and these values are stored in the so-called SATPOS file; this task is done daily.
- The position and velocity vector at any time are calculated by a cubic interpolation using the SATPOS file values; this interpolation is done whenever needed.

The cubic interpolation, between vectors every two minutes, introduces a 3 m error on the position and 0.01 mrad error on the velocity vector direction, which induce errors of the same order of magnitude on the pixel navigation. Such errors are negligible compared to the AVHRR pixel size (about 1km and 1 mrad) and the two-step method has the same accuracy as, for example, the TBUS+BROLYD orbit extrapolation. There is no need to test the cubic interpolation also with Two-Line+SGP4 orbit extrapolation, since interpolation does not rely on the extrapolation model.

A geostationary satellite orbit can be calculated with Two-Line Element sets and SDP4, however this feature is well beyond the scope of AAPP and has not been studied in detail.

8.2.4. NOAA POES Satellite clock error

Before summer 2002

The satellite clock drifts during the life of the satellite. Its error is measured weekly and the clock is periodically reset, when the error becomes too high. Information on the satellite clock is published in the TBUS part IV and consists of four parameters:

- clock error: date and value,
- clock error rate: date and value,
- clock error after last correction: date and value,
- next clock correction: date only.

As the TBUS is delivered daily, the same information is repeated in several successive bulletins. The next clock correction is generally announced well in advance, but the clock error value after the correction is always unknown. At the time of NOAA-11, the reset scheme was regular and rather predictable. This is not true any more.

As for the orbital elements, the clock error information is used after an "ingest" step. This step decodes the TBUS bulletin, controls the information quality and stores the valid information into an historical clock error file, without any duplication of the redundant information. This file is used to obtain the clock error at any time t, as needed for real time or off-line navigation.

The main rules of the quality control and clock error calculation are the following:

quality control

- The clock error at time t is compared to a predicted value at t, derived from the last preceding clock error and clock error rate values and must be close to this predicted value.
- The clock error after last correction is considered as valid in any case.
- The clock error rate must be close to the last preceding one.

clock error calculation

- The clock error at time t is derived from the last values preceding t of the clock error rate and of the clock error, which may be a usual clock error or a clock error after last correction.
- After a clock correction, a zero value is assumed for the clock error, until a clock error after last correction is issued in the TBUS or is manually inserted by the operator.

parameters entered interactively (ignored by the clock information ingest)

- a "null" flag associated to a date, to force a zero value of the clock error for any time after this date; this flag is expected to be used exceptionally, for instance, when several erroneous values occur in the TBUS, making the quality control inefficient.
- a "bias" correction associated to a date, which is added to the clock error for any time after this date. Different bias values can be used during the satellite lifetime. The bias correction is added in any case, even after a clock correction or with a null flag. The bias correction has been introduced because of the clock problem encountered on NOAA-16 and NOAA-15 since September 16, 1999 (see "NOAA-16 Along Track Error", "KLM/ATN Timing Discrepancy - Along Track Anomaly" and "NOAA-15 and 16 Elapsed Time Clock Up" in [19]).

Handling the clock error is a rather complicated process, mainly because erroneous values frequently occur in the TBUS. Furthermore, it should be noted that some of them remain undetected by the AAPP automatic control.

Since summer 2002

NOAA has modified its clock error adjustment method, firstly for NOAA-17 and then for all other NOAA POES. The Satellite Operations Control Center (SOCC) is performing daily clock drift corrections at 23:59:00 UTC for each satellite, in order to reduce the clock error to +/-0.075 second. Therefore processing TBUS clock errors is no longer necessary. The corresponding routines and files

have not been removed from AAPP, in order to allow re-processing of data earlier than 2002. For present data, it is recommended to by-pass any clock error calculation, by introducing a "null" flag and a "bias" correction of 0 in the clock error file of each NOAA satellite.

8.2.5. NOAA POES and MetOp Satellite attitude

The satellite attitude errors induce navigation errors corresponding typically to a few AVHRR pixels. Using a correct attitude value is more important for AVHRR imagery than for HIRS or AMSU imagery.

AAPP has been designed to use an attitude value constant over an HRPT (AHRPT for MetOp) acquisition but varying from one pass to another. The attitude value is supposed to be obtained on an actual AVHRR image by a two-step process:

- locating landmarks in the image to calculate their navigation errors, i.e. the differences between their calculated and true positions in the image
- estimating a satellite attitude error from the landmark navigation errors
- AAPP contains the routines corresponding to the second step, but not to the first one.

The landmark location can be done by the software called ANA-3, i.e. Automatic Navigation Adjustment, version 3 [20]. Such an automatic adjustment has been used operationally at the CMS since 1990 [21]. The software has been re-visited in 2000 to be fully compatible with AAPP and use the precise "World Vector Shoreline" as reference coastline. ANA-3 locates selected coastal landmarks in the AVHRR image, by searching the optimal correlation between small windows in the actual image and the reference landmarks, using channels 1 and 2 for daytime conditions and channels 4 and 5 for nighttime conditions A cloud mask is calculated to reject the too cloudy landmarks, using MAIA routines.

8.2.6. Image navigation

The image navigation converts the line and pixel numbers into latitude and longitude for any pixel of the image, using the satellite parameters previously described.

A necessary step is the conversion of the line and pixel numbers into time and scanning angle, which is based on constant characteristics of the instrument, AVHRR, HIRS, AMSU, MHS or IASI. The instrument values published in section 3 of [1], which are independent on the satellite number, have been used successfully until NOAA-15. Unusual navigation errors have been observed on NOAA-16 imagery and NOAA/NESDIS has recommended some specific corrections (see "Operational Status of NOAA-16 Level 1B" in [19]). These corrections have been put in AAPP, in the so-called "satid" file where the instrument characteristics are defined for each satellite: lower scanning angle step for AVHRR on NOAA-16 and misalignment angles for HIRS-3 on NOAA-16 and NOAA-17. Two corrections have been introduced in AAPP: a lower AVHRR scanning step angle corresponding to a maximum scanning angle of +/-55.25 degree and a 2-degree offset in pixel of the whole HIRS image (NOAA has recommended a 1.8 degree offset, the 2 degree value has been obtained by matching HIRS channel 8 and AVHRR channel 4 images).

The core of the image navigation, which is common to all instruments, is the conversion of the time and scanning angle into latitude and longitude, or direct problem, and the inverse problem.

In the direct problem, the satellite-to-pixel vector is known in the spacecraft-instrument-fixed reference frame; the time is also known and so are all the conversion matrices between the spacecraft-instrument-fixed frame and the Earth-fixed frame. The latitude and longitude are calculated by analytical solution of several equations.

In the inverse problem, which is solved only for cross-track scanning radiometers, the time and, consequently, the conversion matrix are unknown. An iterative resolution is required to calculate the time and scanning angle. The iterative scheme uses convergence criteria corresponding to a position error that is significantly lower than the AVHRR pixel size.

The image navigation uses a satellite attitude constant over the whole image. The method could evolve in order to use a time varying attitude, if the attitude can be calculated at any time by analytical formulas or tabulated values.

8.2.7. Expected accuracy

With the standard options (daily TBUS bulletins, clock error corrected and default satellite attitude), the expected navigation accuracy is about 3 km, in terms of r.m.s. error [17].

In a year of high solar activity (with respect to the 11-year solar cycle), the navigation error may reach 6 to 8 km during a limited period (one or two weeks), corresponding to a phase of intense solar activity, which decreases the orbit prediction accuracy.

Unusual errors of 10 to 15 km may occur on a few passes, due to various reasons: an erroneous clock error value (generally associated with a reset), a satellite attitude anomaly or a very strong solar activity event.

With the Two-Line Element sets, the navigation accuracy is expected to be better than with TBUS bulletins, as shown by an experiment on a 6-month period [22]. This period is not long enough to estimate the navigation accuracy of the Two-Line method in case of high solar activity. More recently, in 2005-2006 the navigation accuracy of NOAA-17 and NOAA-18 has been only slightly better with the Two-lines than with TBUS.

In any case, normal situation or exceptional events, the navigation error is generally a "line" error and not a "pixel" error.

If an automatic adjustment on landmark is used together with AAPP, the expected accuracy is 1.7 km for the passes where this adjustment has been successful [17].

8.2.8. Ephemeris and tracking angles

The AAPP software can also produce useful information for the tracking operations of a ground station:

- an ephemeris file, which contains the times of various events (ascending and descending nodes, start and end of acquisition); there are several types, short term and long term, mono- or multi-satellite,

- a tracking angle file, relative to one station and one satellite, which contains site and azimuth values every second (the site is equal to 90 degree minus the satellite zenith angle).

The **ephe** command produces a short term ephemeris file, i.e. corresponding to duration of the input SATPOS file, which is relative to one satellite and one station. This ephemeris file has the same precision as the image navigation, since the satellite position calculation is based on the SATPOS file with the method presented in section 8.2.3.

The **alleph** command produces the short-term ephemeris and tracking angle files, for one station and several satellites. It also merges the mono-satellite ephemeris files into a multi-satellite ephemeris file where the acquisition conflicts (two satellites passing simultaneously) have been identified and one satellite has been chosen according to priority rule. Here again, the satellite position is calculated with the SATPOS file and all files have the same precision as the image navigation.

AAPP can also produce a long-term ephemeris, i.e. over several months, for one satellite and several stations. In that case, the satellite position is calculated by an approximate method: circular orbit with linear variation of the nodal period and of the node longitude increment. This method is definitely less precise than using SATPOS for a two or three day extrapolation, but its error increases very slowly with time. So, a long-term ephemeris can be used to prepare a planning or an experiment schedule. The long-term ephemeris is produced by two commands:

- **lgepheing**, which ingests a TBUS, extracts the parameters that are ephemeris-related (mainly the nodal period and node longitude increment) and stores them into an historical file.
- **lgephe** , which creates the long-term ephemeris file.

8.3. <u>CALIBRATION</u>

All the referenced data and all the calibration procedures are detailed in reference [1] for each instrument and [23] for the HIRS calibration algorithm version 4.

8.3.1. <u>Thermal field : Background.</u>

At equilibrium state, the radiative field is only temperature dependent, non-polarised and isotropic. The field is characterised by its monochromatic radiance (or black body radiance) R_σ (W.m^{-2}.sr^{-1}.cm) at temperature T(K). Taking into consideration that radiative emission is due to electrical oscillators whose energy is quantified (h ν integer multiple), Planck's law is expressed as:

$$R_\sigma(T) = B(\sigma, T) = \frac{2hc^2\sigma^3}{e^{\frac{hc\sigma}{kT}} - 1}$$

with :

$h = 6.6261 \times 10^{-34}$ J.s, Planck constant.
$c = 3 \times 10^8$ m.s^{-1}, light velocity.
$k = 1.38 \times 10^{-23}$ J.K^{-1}, Boltzmann constant.
σ = wave number in cm^{-1}.
$B(\sigma, T)$ = Planck's function.

where the temperature is extracted by inverting the previous relation:

$$T = \frac{C_2\sigma}{\ln\left(1 + \frac{C_1\sigma^3}{R_\sigma}\right)}$$

with : $C_1 = 1.191 \times 10^{-5}$ mW.m^{-2}.sr^{-1}.cm^4
$C_2 = 1.439$ K.cm.

8.3.2. <u>Calibration principle</u>

The calibration procedure establishes a relation between the sensor output measured on a n-bits dynamic range (2^n possible values) and the associated physical parameters, i.e. between the observed scene radiance and the corresponding numeric counts. Figure 8 illustrates the IR measurement principle.
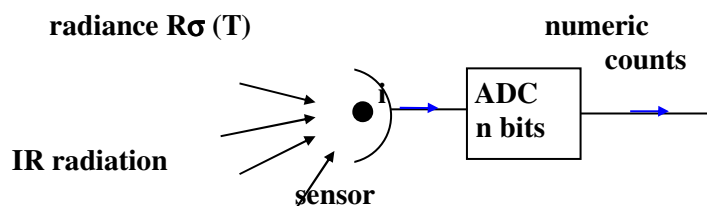
Figure 8: One IR channel for radiance measurements.

This relation depends on each spectral channel and on the temperature of the whole set up. The thermal channels (IR and μ-wave) are calibrated with the help of a warm black body target (where the radiance versus temperature follows Planck's law), and with a cold target (usually the cold space view). The visible channels are calibrated using halogen lamps. A pre-launch calibration procedure exists for all channels. The measured radiance is converted into brightness temperature by inverse Planck's law application.

8.3.3. HIRS and AVHRR visible channels calibration for albedo determination (AVHRCL and HIRSCL)

The VIS calibration performs the conversion of numeric counts into albedo (in percent). This quantity is calculated applying the linear function:

$$Ai = GiX + Ii$$

with Ai = albedo percentage
   Gi = channel i gain
   X = numeric counts from measurements on channel I
   Ii = albedo offset for a zero numeric count.

Gains and offsets are measured and referenced before the satellite launch for each VIS channel. An integrating sphere is used as illumination source for the calibration procedure.

The sphere equipped with 20 halogen quartz lamps is calibrated: the spectral radiance emerging from the sphere versus the number of turned on lamps, is determined. The result is a calibration curve where the spectral radiance varies over three orders of magnitude from black (all lamps turned off) to the maximum level of illumination (all lamps turned on). Each instrument channel is illuminated by the light emerging from the sphere, and integrates the sphere output radiance according to the own spectral channel bandwidth. The maximum in-band radiance (20 lamps switched on) is noted $R\sigma_l$. In flight, each channel integrates an $R\sigma_s$ radiance due to the reflected solar radiation at the top of the atmosphere. The albedo percentage is defined as the ratio:

$$A = 100\frac{R\sigma_s}{R\sigma_l}$$

To convert the albedo percentage into spectral radiance R_λ (W.m^{-2}.sr^{-1}.μm^{-1}), the following relation is applied:

$$R_\lambda = \frac{AF}{100\pi W}$$

with : F = integrated and weighted (channel spectral response function) solar flux (W.m^{-2}).

   W = spectral channel bandwidth (μm).

Some channels (VIS and near IR) are known to degrade in orbit, which means that the pre-launched calibrated values evolve slowly over time. Because of the absence of on board calibration devices for the VIS channels, other in flight calibration techniques based on the observation of radiometrically

stable terrestrial calibration target sites (ice, desert...) can be used, after some corrections for atmospheric effects.

The calibration coefficients values are listed in reference [1], and read from the *avhcal.txt* (AVHRR) and *calcoef.dat* (HIRS) or *h_calcoef_algoV4.dat* (HIRS calibration algorithm version 4) parameters files for the AAPP calibration procedure. These coefficients are stored in the level1b files: *hrptl1b*, and *hirsl1b*. The AAPP operational scheme keeps the coefficient values in agreement with the pre-launch coefficients given by NOAA on the web site of the NOAA user's guide [1].

NOAA also maintain "operational" visible calibration coefficients for AVHRR, and the script *avh_get_vis_coefs* can be used to download the files and append the coefficients to level 1B files.

8.3.4. AVHRR thermal channels calibration (AVHRCL)

The pre-launch calibration procedure establishes a relation between the thermal channels numeric counts and a calibrated black body radiance source. This relation is linear for channel 3 (InSb sensor), but not for channels 4 and 5 (HgCdTe sensor). Non-linearity corrections must be applied for numeric counts to radiance conversion.

After the satellite launch, the results of the calibration performed on the ground can't be applied anymore, because the radiometer characteristics change. The thermal channels are then calibrated in flight, periodically, by radiance measurements on reference sources as space (sp - cold target), and as on board black body (bb - warm target) whose temperature is determined by platinum resistance thermometers (PRT). (The variation of the resistance is a function of temperature, so the current through the PRT varies and is converted into numeric counts to be introduced into the HRPT format). For each spectral channel, a calibration curve is established with the help of the two referenced measurements on the cold and warm targets. Any radiance corresponding to any given numeric count can then be deduced from this curve.

An example of calibration curve is shown on Figure 9.
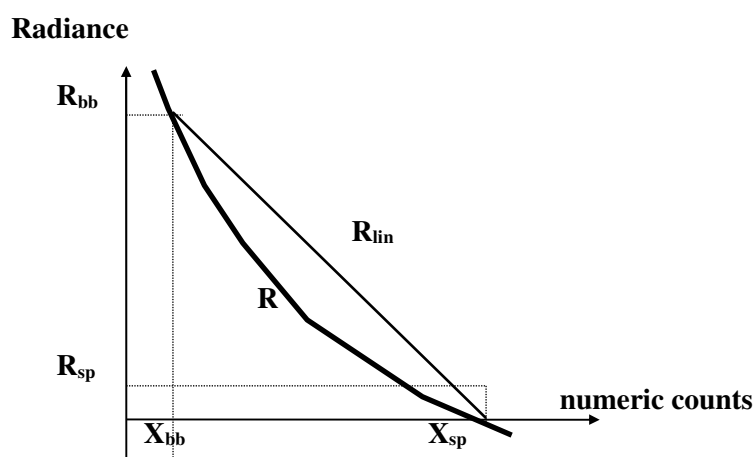
Figure 9: Calibration curve (radiance as a function of the numeric counts).

The radiance is converted into brightness temperature by application of the inverted Planck's formula.

To determine the reference black body radiance, its temperature has to be measured. This task is performed by the PRT numeric counts extraction on the 4 platinum resistances, two of the PRT temperatures being colder than the other two. For one PRT, the temperature (K) is given by the conversion relation (PRT numeric count to temperature):

$$T_i = \sum_{j=0}^{4} a_{ij} (PRT_i)^j$$

with : T_i = PRT number i temperature

a_{ij} = conversion coefficient

PRT_i = mean numeric counts associated to PRT number i.

The reference black body temperature T_{bb} (K) is determined by averaging the temperatures derived from the 4 PRTs:

$$T_{bb} = \sum_{i=1}^{4} b_i T_i$$

with : b_i = weighted coefficient.

a_{ij} and b_i coefficients are referenced in document [1] for each PRT, and in the *avhcal.txt* parameters file for the AAPP calibration task.

The expression for black body radiance R_{bb} at temperature T_{bb}, is established using the Planck formula $B(\sigma,T)$, and taking into account the AVHRR spectral channels response function $\Phi(\sigma)$:

$$R_{bb} = \frac{\sum_{i=1}^{n} B(\sigma_i, T_{bb})\Phi(\sigma_i)\Delta\sigma}{\sum_{i=1}^{n} \Phi(\sigma_i)\Delta\sigma}$$

with : $\Delta\sigma = \sigma_{i+1} - \sigma_i$ = spectral interval for calculation.

$\Delta\sigma$ and $\Phi(\sigma_i)$ are specified in document [1] for each thermal channel, and in the *avhcal.txt* parameter file for the AAPP calibration task.

Each channel gives a mean (associated to several target observations) numeric count X_{bb} corresponding to R_{bb}.

The cold reference is given by the space radiance R_{sp}. During this measurement, the radiometer scanning mirror is turned toward space, and doesn't look at the Earth. Each channel gives the corresponding X_{sp} numeric counts.

Notes: The PRT numeric counts are included in the HRPT format. The numeric counts for a given PRT are given every 5 minor frames:

HRPT minor frame	parameter

n	REF (for synchro.)
n+1	PRT1
n+2	PRT2
n+3	PRT3
n+4	PRT4

Table 4: PRT$_i$ numeric counts occurrence.

One PRT mean temperature is calculated with 11 measurement samples (representing 55 minor frames for the 4 PRTs).

Linear approximation: From (R$_{bb}$, X$_{bb}$) and (R$_{sp}$, X$_{sp}$), the equation of the calibration curve is easily established for each linear channel:

$$R_{lin} = GX + I$$

with : $\quad G = (R_{bb} - R_{sp}) / (X_{bb} - X_{sp})$

$\qquad I = R_{sp} - G.X_{sp}$

R$_{lin}$ is the radiance corresponding to X numeric counts associated to Earth observation.

Non linearity corrections: are directly applied on the R$_{lin}$ radiance:

$$R = aR_{lin} + bR_{lin}^2 + c$$

a, b and c are referenced in document [1] for each non linear AVHRR channel, and in the *avhcal.txt* parameters file for AAPP calibration task.

Introducing the R$_{lin}$, G and I expressions in R formulation, one can deduce a direct relation between R and the corresponding numeric counts X:

$$R = k1X^2 + k2X + k3$$

with : $\quad k1 = b.G^2$

$\qquad k2 = a.G - 2.k1.X_{sp} + 2.b.G.\, R_{sp}$

$\qquad k3 = c + a.\, R_{sp} - a.G.X_{sp} + b.(\, R_{sp} - G.\, R_{sp})^2$

These calibration coefficients are stored in the level1b *hrptl1b* file. The numeric counts X are converted into radiances using the previous relation. The radiances are converted into brightness temperatures using the inverted Planck's law. These results are reported in the level1c file.

Note: The calibration coefficients are calculated for each scan line. This calibration method is valid for AVHRR/2 and AVHRR/3.

Values of parameters useful for computing calibration parameters are written to a file *monavhr.txt*. This historical file allows the study of the target counts, space counts and PRT counts, so that the instrument health can be checked. The AAPP user has to create his own tools to study the values written in the file. The data format is described in the AAPP data format document.

8.3.5. HIRS thermal channels calibration: First algorithm available in AAPP (HIRSCL)

The thermal channels are calibrated in flight, by radiance measurements on reference sources each 40 scan lines. For HIRS/2, 3 or 4 calibration lines are then introduced to produce numeric counts corresponding to space radiance (sp - cold target), and to the radiance of two on-board black bodies (bb - one warm and one cold target) whose temperature is determined by platinum resistances (PRT). However, the bb cold target temperature is not used in the computation, because of the large temperature gradients induced by solar contamination. For HIRS/3 and 4, there are only 2 calibration lines, one for space and one for the on-board warm bb target.

For each spectral channel, a linear calibration curve is established with the help of the two referenced measurements on the cold space and on the warm target. Any radiance corresponding to Earth observation numeric counts can then be deduced from this relation.

To determine the reference black body radiance, its temperature has to be measured. This task is performed by the PRT numeric counts extraction on the 4 platinum resistances for HIRS/2 or 3, on the 5 platinum resistances for HIRS/4. For one PRT, the temperature (K) is given by the conversion relation (PRT numeric count to temperature):

$$T_i = \sum_{j=0}^{5} a_{ij} (PRT_i)^j$$

with : T_i = PRT number i temperature

a_{ij} = conversion coefficient
PRT_i = mean numeric counts associated to PRT number i.

The reference black body temperature T_{bb} (K) is determined by averaging the temperatures derived from the 4 or 5 PRTs.

a_{ij} coefficients are referenced in document [1] for each PRT, and in the *calcoef.dat* parameters file for the AAPP calibration task.

5 PRT_i measurements performed during the calibration line of the warm target, plus 5X measurements of the PRT_i from X calibration lines around the warm target, are used in the calculation of a PRT mean numeric counts (PRT_i). The X value is written in *testcoef.dat* file. For each calibration cycle (every 40 scan lines), the mean numeric counts PRT_i results from the averaging of 5*(2X+1) measurements on the target.

The black body radiance R_{bb} at T_{bb} temperature, is established using the Planck's law:

$$R_{bb} = B(\sigma_c, T_{bb}^*)$$

with : σ_c = central wave number

$T_{bb}^* = b + c.T_{bb}$ effective temperature with band correction.

b and c are referenced in document [1] for each channel, and in the *calcoef.dat* parameter file for the AAPP calibration task.

For each channel, average values of numeric counts X_{bb} (of several target observations) corresponding to R_{bb} and of X_{sp} corresponding to R_{sp} are determined. The computation of the mean numeric counts requires that the 56 calibration line samples are filtered and bad values eliminated (the test parameters are available in *calcoef.dat* and *testcoef.dat* files). This is necessary because the 8 first space views are polluted by the movement of the radiometer (while the 56 samples are correct for the bb target, but the 8 first bb views are also rejected for the homogeneity question). Finally, 48 samples are processed for space and black body target.

Thanks to (R_{bb}, X_{bb}) and (R_{sp}, X_{sp}), the equation of the calibration curve is easily established for each linear channel:

$$R = GX + I$$

R is the radiance corresponding to X numeric counts associated to Earth observation.

The slope $G = (R_{bb} - R_{sp}) / (X_{bb} - X_{sp})$ and the intercept $I = R_{sp} - G.X_{sp}$ are the calibration coefficients relative to the calibration lines cycle. For every scan line containing Earth view data (between the calibration cycles), new (G,I) coefficients are calculated using a linear interpolation of the coefficients of the two surrounding calibration cycles. These coefficients are stored in the level1b *hirsl1b* file. For each channel, the mean (G,I) calibration coefficients are calculated and stored in the header of the *hirsl1b* file. The radiances are converted into brightness temperatures using the inverted Planck's law. These results are reported in the level1c file.

Values of parameters useful for computing calibration parameters are written to a file *monhirs.txt*. This historical file allows the study of the target counts, space counts and PRT counts, so that the instrument health can be checked. The AAPP user has to create his own tools to study the values written in the file. The data format is described in the AAPP data format document.

8.3.6. HIRS thermal channels calibration: Second algorithm available in AAPP (HIRSCL_ALGOV4)

Intoduction

This algorithm doesn't work for data of pre-NOAA-K satellites. It was developed to manage the HIRS calibration algorithm version 4.0 of the NOAA and described in [23] and [24]. It is also useful to refer to the NOAA KLM User's guide Section 7.2 [1].

This algorithm was developed in AAPP to be very similar to the calibration process of NOAA – the aim being to have consistency between local data and global data. Nevertheless the main difference between the AAPP algorithm and the NOAA algorithm is for the average data (average slopes and B1, coefficients of correlation between the telescope temperature and calibration intercept) NOAA uses 24 hour averages. These are not available from local data, so the average slopes and B1 are computed from past data. The past data are taken from the reference date minus x hours to the reference date. By default, the reference date is the date of the current orbit, x is defined by the AAPP user (see ATOVS_ENV).

The second main difference is that the AAPP algorithm does not control the moon contamination on the space views. This will be done in a future version of AAPP.

The choice of flagging some bits in the level 1b could also be different.

Note that the new algorithm has been validated using a limited amount of NOAA-KLM HIRS data.

Principle

The HIRS thermal channels are calibrated in flight, by radiance measurements on reference sources each 40 scan lines (256 seconds). For HIRS/3 or 4 the reference sources are a space scan line and an on-board blackbody (BB) or internal warm target (IWT) scan line. For each spectral channel, a

calibration curve is established with the help of the two referenced measurements on the cold space and on the warm target. Any radiance corresponding to any Earth observation numeric counts can then be deduced.

It is assumed that radiance can be related to counts through the quadratic equation:

$$R = a_0 + a_1*CN + a_2*CN^2 \qquad (1)$$

With R = radiance

CN = output in counts from the view

a_0, a_1, a_2 = calibration coefficients

Assuming that a_2 is computed before launch and is an unchanging characteristic of the channel, a_0 and a_1 can be determined if we apply equation 1 to simultaneous views of space and blackbody (warm target) source:

From
$$R_{sp} = a_0 + a_1*CN_{sp} + a_2*CN_{sp}^2$$
$$R_{bb} = a_0 + a_1*CN_{bb} + a_2*CN_{bb}^2$$

With R_{sp} = radiance of the space (the assumption is made that $R_{sp} = 0$)

R_{bb} = radiance of the black body views

CN_{sp} = mean count from the views of space

CN_{bb} = mean count from the views of black body

We get
$$a_1 = [R_{bb} - a_2 (CN_{bb}^2 - CN_{sp}^2)] / (CN_{bb} - CN_{sp}) \qquad (2)$$
$$a_0 = - a_2 CN_{sp}^2 - a_1 CN_{sp} \qquad (3)$$

a_1 is the slope, a_0 the intercept.

The aim of this calibration task is to compute the slope and the intercept.

Step 1: For each internal blackbody view scan line, determine the blackbody temperature and for each IR channel, the radiance (R_{bb}):

To determine the reference blackbody radiance, its temperature has to be measured. This task is performed by the numeric counts extraction on the 4 platinum resistance thermometers (PRT) for NOAA-KLM and the 5 PRTs for NOAA-N. For one PRT, the temperature is given by the conversion relation (PRT numeric count to temperature):

$$T_i = \sum_{j=0}^{5} a_{ij} (PRT_i)^j$$

with : T_i = temperature of the PRT number i, a_{ij} = conversion coefficient

PRT_i = mean of the numeric counts associated to PRT number i.

aij coefficients are referenced in document [1] for each PRT, and in the h_calcoef_algoV4.dat parameters file for the AAPP calibration task.

5 PRTi measurements are performed during the calibration line of the warm target. 2*5X measurements of the PRTi from X calibration lines around the warm target scan line are also used in the calculation of a PRT mean numeric counts (PRTi).(X in h_testcoef_algoV4.dat file).

The 5*(2X+1) PRTi measurements are checked:

the difference between the maximum PRTi measurement value and the minimum one must be less than a limit prtminmax (in h_testcoef_algoV4.dat file)

the minimum number of valid PRTi measurements to compute a mean is prtminnb (in h_testcoef_algoV4.dat file)

The mean numeric count PRTi results from the averaging of valid measurements.

The reference blackbody temperature Tbb is determined by averaging the temperatures derived from the 4 or 5 PRTs. If only one or zero temperatures are computed, the reference blackbody temperature is declared bad. The calibration cycle is declared unqualified.

The blackbody radiance Rbb at Tbb temperature is established using the Planck's law:

$$R_{bb} = B(\sigma_c, T_{bb}^*)$$

with : σ_c = central wave number

$T_{bb}^* = b + c.T_{bb}$ effective temperature with band correction.

b and c are referenced in document [1] for each channel, and in h_calcoe_algoV4.dat parameter file for AAPP calibration task.

Step 2: For each calibration cycle and for each IR channel, compute the averaged output counts for the space views and for the internal blackbody views

At each calibration cycle and for each thermal channel, an average value of numeric counts CN_{bb} corresponding to R_{bb} and of numeric counts CN_{sp} corresponding to R_{sp} is determined.

The HIRS instrument has contamination in the first xx FOVs of the space scan (xx in *h_testcoef_algoV4.dat* file), polluted by the movement of the mirror. For consistency, the same xx FOVS are eliminated from the scan line of the warm target.

Finally, (56-xx) samples are processed for space and for blackbody target.

The samples are checked:

Samples with counts that are outside the gross limits are removed.

The mean and the standard deviation of the remaining samples are computed if the samples are numerous enough.

The standard deviation is compared to the NEDC specification with

NEDC = abs(NEDN / average_slope).

NEDN: the noise equivalent delta radiance is referenced in document [1] for each channel, and in *h_calcoe_algoV4.dat* parameter file for AAPP calibration task.

The average slope is computed before the calibration run with calibration data from previous orbits. See the introduction of this paragraph.

If STD < NEDC, all samples pass the test. Then the samples that are outside of 3 sigma are removed. The mean and the standard deviation are recomputed. The recomputed mean will be used for further processing.

If STD > NEDC, the median value of the samples is computed and will be use for further processing.

If the averaged output counts for the space views or for the internal blackbody views can't be computed, the calibration cycle is declared unqualified.

Step 3: For each calibration cycle and for each IR channel, compute the BB (or raw) slope and intercept.

From equation 2 and 3 (see above) and assuming that a_2 is equal to zero in this algorithm :

$a_1 = R_{bb} / (CN_{bb} - CN_{sp}) = S$ (BBslope S)

$a_0 = -a_1 CN_{sp} = I$ (BBintercept I)

The quality of the BBslope is controlled:

First, each BBslope is checked to ensure that its value is within a threshold from their mean value. If not, the one furthest from the mean value is removed and the mean is recomputed. The process continues till the condition is satisfied.

Then, each BBslope is checked against the average slope (see step 2, NEDC test). If it deviates from the average slope by more than a threshold it is considered an anomaly. If the slope is anomalous, the intercept is also suspect. The calibration cycle is declared unqualified.

Step 4 : For each Earth view scan line and for each channel, compute the slope.

A super-swath is defined as 40 scan-lines of HIRS data that start with a calibration cycle (1 space view line, 1 internal blackbody view line), followed by 38 Earth view scan lines.

For a normal super-swath k (in the middle of an orbit for example), the calibration slope for the 38 Earth view scan lines of the current super-swath k is the running average of 3 values: the BB slope of calibration cycle(k), the BB slope of calibration cycle(k-1), the BB slope of calibration cycle(k-2).

```
   Calib cycle k-2      Calib cycle k-1      Calib cycle k
   ----------| |----------------------| |----------------------| |-------------
                         current super-swath k
```

$S'(k-1:k) = [S(k-2) + S(k-1) + S(k)] / M$

With

K the current super-swath number

S'(k-1:k) the running average of the 3 slopes, to be used for the 38 Earth view scan lines in the current super-swath k.

S(k-2) the BB slope for the calibration cycle (k-2)

S(k-1) the BB slope for the calibration cycle (k-1)

S(k) the BB slope for the calibration cycle (k)

M the number of qualified BB slopes (see previous step) used for averaging (M=1 to 3)

Note that the current super-swath number k includes the 2 lines of the calibration cycle k-1 and not the 2 lines of the calibration cycle k.

For a partial super-swath k (when an orbit does not begin or end with a complete calibration cycle or when the data stream is broken in the middle of an orbit for example), the calibration slope for the 38 Earth view scan lines of the current super-swath k is the average value of the qualified slopes from the nearest 2 (or at least 1) calibration cycles. If neither value is qualified, the calibration slope for the 38 Earth view scan lines of the current super-swath k is the average slope computed with the data of the previous orbits (see the introduction of this paragraph). If the average slope is equal to zero or is missing, the calibration slope for the 38 Earth view scan lines of the current super-swath k is also missing.

Step 6 : For each calibration cycle and for each channel, recompute the intercept

The intercept is recomputed using the average slope derived in the previous step. As the space view line of the calibration cycle (k-1) belongs to the super-swath k, the equation is:

$$I'(k-1) = -S'(k-1:k)*CN_{sp}(k-1)$$

With   *I'(k-1)* The recomputed intercept for the calibration cycle (k-1)

            S'(k-1:k) The average slope for the current super-swath (k) (lines between the calibration cycles (k-1) and (k)).

            $CN_{sp}(k-1)$ The space view count average for the calibration cycle (k-1)

If $CN_{sp}(k-1)$ is bad , the intercept is recomputed using the data of the blackbody view line.

$$I'(k-1)= R_{bb}(k-1) - S'(k-1:k)*CN_{bb}(k-1)$$

With   *I'(k-1)* The recomputed intercept for the calibration cycle (k-1)

            $R_{bb}(k-1)$ The radiance of the internal blackbody for the calibration cycle (k-1)

            S'(k-1:k) The average slope for the current super-swath (k) (lines between the calibration cycles (k-1) and (k)).

            $CN_{bb}(k-1)$ The internal blackbody view count average for the calibration cycle (k-1)

If $CN_{bb}(k-1)$ or $R_{bb}(k-1)$ are bad , the intercept is declared bad.

Step 7 : For each Earth view scan line and for each channel, compute the intercept

If the slope is essentially constant, the intercept varies appreciably throughout an orbit.

The HIRS instrument measures all radiation falling on the detector. To minimize false fluctuations in the signals, the instrument temperature is carefully controlled, so that most optical components experience temperature changes very slowly with respect to the times between two calibration cycles (256 seconds). However, the baffle (identified as the secondary mirror) is a blackened light material which is subject to short-term temperature changes from emission or blackbody radiation and absorption of incident radiation from the internal warm target source, space and the variable Earth views. So the baffle affects all measurements on a time scale of seconds and this must be accounted for. [1]

So, the intercept is defined at an Earth view scan line by:

$$I''(n) = Il(n) + \beta \, It(n)$$

With n The scan line number in the super-swath (k) numbered 2-39
                    (n is an Earth scan line between the calibration cycle (k-1) and (k), n=0 for the
                     space line, n=1 for the BB line))
          $Il(n)$ The linear interpolation of the intercept between two calibration cycles
          $It(n)$ The correction to the intercept based on the secondary mirror temperature
          β The switch. When ß equal to zero, no term based on the secondary mirror
                 temperature is applied (see the option in ATOVS_ENV).

$Il(n)$ is computed as :

$$Il(n) = I''(k-1) + n \cdot (I''(k) - I''(k-1)) / 40$$

With n The scan line number in a super-swath (k) numbered 2-39
                  (n is an Earth scan line between the calibration cycle (k-1) and (k))
        $I''(k-1)$ The recomputed intercept at calibration cycle (k-1) (see below)
        $I''(k)$ The recomputed intercept at calibration cycle (k) (see below)

$I''(k-1)$ and $I''(k)$ are the intercepts computed with the same slope S'(k-1:k).
So $I''(k-1) = I'(k-1)$ computed in the previous step
    $I''(k) = \alpha * I'(k)$ With α the correction
                               $\alpha = S'(k-1:k) / S'(k:k+1)$

For Earth scan lines located before the first qualified calibration cycle:
        $Il(n) = I'(1)$
For Earth scan lines located after the last qualified calibration cycle:
        $Il(n) = I'(k)$
        With k, number of the last qualified calibration cycle

$It(n)$ is computed as :
        $It(n) = b_1 \cdot [(T'(n) - T'(k-1)) - n \cdot (T'(k) - T'(k-1))/40]$

    With

n The scan line number in a super-swath (k) numbered 2-39
        (n is an Earth scan line between the calibration cycle (k-1) and (k))

$T'(n)$ The secondary mirror temperature "prime" at scan line n

$T'(k-1)$ The secondary mirror temperature "prime" at the space view scan line of
       the calibration(k-1) (see below)

$T'(k)$ The secondary mirror temperature "prime" at the space view scan line of the
       calibration (k) (see below)

b_1 The correlation coefficient between the secondary mirror temperature and
       calibration intercept for a given channel.

For Earth scan lines located before the first qualified calibration cycle:

$$It(n) = b_1 \,[\, T'(n) - T'(1) \,]$$

For Earth scan lines located after the last qualified calibration cycle:

$$It(n) = b_1 \,[\, T'(n) - T'(k) \,]$$
With k the number of the last qualified calibration cycle

$b1$ is computed before the calibration run with calibration data from previous orbits. See the introduction of this paragraph. b1 is separated by Night and Day (b1n, b1d) and all conditions (b1) (user option in ATOVS-ENV)

$T'(n) = T(n-1) + 0.4609 * [\, T(n) – T(n-1) \,]$
With $T'(n)$ the linearly interpolated to the midpoint of the radiometric data (beam position 28.5)
    n the line number in the super-swath
    $n-1$ the previous line number
     T the secondary mirror temperature
For the first line of the orbit:
$T'(1) = T(1) – 0.5391 * [\, T(2) – T(1) \,]$

For every scan line : $T(n) = \displaystyle\sum_{i=0}^{5} a_i (CNs)^i$

With : n the line number in the super-swath

    $T(n)$ the secondary telescope temperature at the line number n

    a_i the conversion coefficients

    CN_s the numeric count associated to the secondary telescope temperature.

Step 8 :Values of parameters useful for computing calibration parameters are written to a file _hirs_historic.txt_.

This historical file allows the study of the target counts, space counts and PRT counts, so that the instrument health can be checked. The AAPP user has to create his own tools to study the values written in the file. The data format is described in the AAPP data format document.
A script was created to manage this file that can be very big (_hirs_historic_file_manage.ksh_)

The HIRS level1B file is updated:

At each blackbody view line, the BB slopes (_S_) and BB intercepts (_I_) are stored as primary and secondary calibration coefficients.

At each space view line, the recomputed slopes (*S'*) and the recomputed intercepts (*I'*) are stored as primary and secondary calibration coefficients.

At each Earth view line, the recomputed slopes (*S'*) and the final intercepts (*I''*) are stored as primary calibration coefficients.

At each Earth view line, the recomputed slopes (*S'*) and the linear intercepts (*Il*) are stored as secondary calibration coefficients.

The average slopes and the *b1* coefficients used are stored in the level 1b header.

8.3.7. MSU µ-waves channels calibration (MSUCL)

The calibration is performed by radiance measurements on reference sources at each scan line. The numeric counts corresponding to space (sp) and 2 on-board black body (bb) radiances, are recorded. A couple of platinum resistance thermometers (PRT) are dedicated to the temperature measurement of each warm target. Each scan line has its own calibration coefficient set. However, the calibration coefficients that have to be applied to convert numeric counts into radiance (concerns all the lines scanned during the same orbit), are computed averaging the slope and intercept of each scan line. This means that there is only one set of calibration coefficients for all the lines covered by the orbit.

The MSU sounder has 2 on-board warm targets. The target number 1 (bb1) is viewed by channels 1 and 2. The target number 2 (bb2) is viewed by channels 3 and 4. Each of the on-board warm targets has 2 PRTs to determine their temperature (PRT1A and PRT1B for bb1, PRT2A and PRT2B for bb2). The conversion of each PRT count output to temperature requires 2 calculation steps: one PRT numeric counts ($X_{A/B}$) $\rightarrow$ to resistance ($R_{A/B}$) $\rightarrow$ to temperature ($T_{A/B}$).

1st step: $X_{A/B} \rightarrow R_{A/B}$ conversion of A or B PRT system is expressed by the following relations:

$$R_A = k_0 + k_1 \frac{X_A - T_{A-CALLO}}{T_{A-CALHI} - T_{A-CALLO}}$$

$$R_B = k_0 + k_1 \frac{X_B - T_{B-CALLO}}{T_{B-CALHI} - T_{B-CALLO}}$$

with : R_A = PRT1A or PRT2A resistance

R_B = PRT1B or PRT2B resistance
X_A = PRT1A or PRT2A numeric counts
X_B = PRT1B or PRT2B numeric counts
$T_{A-CALHI}$, $T_{A-CALLO}$, $T_{B-CALHI}$, $T_{B-CALLO}$ are high and low calibration reference points for electronics systems A and B respectively.
k_0 and k_1 coefficients are referenced in document [1], and in *calcoef.dat* parameters file for the AAPP calibration task.

2nd step: The target bb1 temperature (K) is the average of the 2 temperatures derived from PRT1A and PRT1B.The target bb2 temperature (K) is the average of the 2 temperatures derived from PRT2A and PRT2B. $R_{A/B} \rightarrow T_{bb1/bb2}$ conversion is determined by the following relation:

$$T_{bb1/bb2} = \frac{1}{2}\left(\sum_{i=0}^{2} e_i R_A^i + \sum_{i=0}^{2} e_i R_B^i\right)$$

The e_i coefficients are referenced in document [1], and in *calcoef.dat* parameters file for the AAPP calibration task.

The black body radiance R_{bb} at temperature T_{bb} is established using the Planck's law:

$$R_{bb} = B(\sigma_c, T_{bb})$$

with σ_c = central wave number (referenced in document [1] for each channel, and in *calcoef.dat* parameter file for AAPP calibration task).

Non linearity corrections of output counts: The relationship between input radiance and MSU channels output counts $R = f(X)$ is not linear. A correction algorithm must be applied on the numerical counts X:

$$X' = \sum_{i=0}^{2} d_i X$$

with X' = modified count value to be used in the linear relationship $R = G. X' + I$

d_i is the non-linearity correction coefficients referenced in document [1] (provided by pre-launch measurement), and in *calcoef.dat* parameters file for the AAPP calibration task.

Thanks to (R_{bb}, X'_{bb}) and (R_{sp}, X'_{sp}), the equation of the calibration curve is easily established for each linear channel:

$$R = GX' + I$$

with : $G = (R_{bb} - R_{sp}) / (X'_{bb} - X'_{sp})$

$I = R_{sp} - G. X'_{sp}$

R is the radiance corresponding to X' corrected numeric counts.

The (G,I) calibration coefficients are stored in the level1b *msul1b* file. The radiances are converted into brightness temperatures using the inverted Planck's law. These results are reported in the level1c file.

Values of parameters useful for computing calibration parameters are written to a file *monmsu.txt*. This historical file allows the study of the target counts, space counts and PRT counts, so that the instrument health can be checked. The AAPP user has to create his own tools to study the values written in the file. The data format is described in the AAPP data format document.

8.3.8. AMSU-A / AMSU-B / MHS µ-wave channels calibration (AMSUnCL/ MHSCL)

AMSUACL, AMSUBCL and MHSCL compute the calibration coefficients for AMSU-A, AMSU-B and MHS. The procedure is similar for the 3 sounders, except for a few minor differences such as the number of PRTs and warm targets. The warm target temperatures are determined with the help of 5 PRTs for AMSU-A (A1-1) channels: 3-15, 7 PRTs for AMSU-A (A1-2) channels: 1-2, and 7 PRTs for all AMSU-B channels: 16-20. MHS has 5 PRTs. There are different black body targets for each subsystem channel. The cold reference is space.

The pre-launch calibration procedure permits a relation to be established between the μ-wave channels numeric counts and a calibrated black body radiance. This relationship is not linear due to imperfect square law detectors. A band correction is also necessary for channels 19 and 20, since the monochromatic assumption breaks down for warm targets radiance measurement.

To determine the reference black body radiance, its temperature has to be measured. This task is performed by extracting the PRT numeric counts. For one AMSU-A or AMSU-B PRT, the temperature (K) is given by the conversion relation (PRT numeric count to temperature):

$$T_i = \sum_{j=0}^{3} f_{ij}(PRT_i)^j$$

with: T_i = PRT number i temperature

f_{ij} = conversion coefficient
PRT_i = mean numeric counts associated to PRT number i.

MHS uses a different measurement technique (based on a constant current source), necessitating a two-stage procedure. Three precision reference resistors are used to calibrate the relationship between counts and resistance, via a least-squares straight line fit – the same relationship being used for all PRTs. Then the resistance, R_i for each PRT is converted to temperature via the calibration constants of the PRT:

$$T_i = \sum_{j=0}^{3} f_{ij}R_i^{\ j}$$

MHS is further complicated by the fact that it has a redundant Processing Interface Electronics unit (known as PIE-B), with separate PRTs and reference resistors.

For both AMSU and MHS the reference black body temperature T_{bb} (K) is determined by a weighted average of all PRT temperatures:

$$T_{bb} = \frac{\sum_{i=1}^{m} w_i T_i}{\sum_{i=1}^{m} w_i} + \Delta T_{bb}$$

with : w_i = weighted coefficient

ΔT_{bb} = warm load correction factor for each channel
m = number of PRTs (5 or 7) depending on the warm target.

Similary, a cold space temperature correction ΔT_{sp} is provided, because the space view is contaminated by radiation emitted by the spacecraft platform itself: $T_{sp} = 2.73\ (K) + \Delta T_{sp}$.

A band correction is applied for channel 19 and 20: $T_{bb}^{\ *} = b + c.T_{bb}$.

The black body radiance R_{bb} at T_{bb} or $T_{bb}^{\ *}$ temperature, is established using the Planck's law:

$$R_{bb} = B(\sigma_c, T_{bb})\ \ or\ B(\sigma_c, T_{bb}^{\ *})$$

with : σ_c = central wave number.

f_{ij} and w_i, b and c coefficients, and temperature offsets are referenced in document [1] for each PRT, and in *amsua_clparams.dat*, *amsub_clparams.dat* and *mhs_clparams.dat* parameters files for the AAPP calibration task.

The calibration coefficients are calculated for every scan line. For each channel an average value (from 2 samples for AMSU-A and 4 samples for AMSU-B and MHS) for numeric counts X_{bb} corresponding to R_{bb} is computed. Space radiance R_{sp} is used as the cold reference. Each channel gives an average value (from 2 samples for AMSU-A and 4 samples for AMSU-B) for numeric counts X_{sp} corresponding to R_{sp}.

__Non linearity corrections:__ From (R_{bb}, X_{bb}), (R_{sp}, X_{sp}) and non linearity coefficients (u), the equation of the calibration curve L = f(X) is established by the relationship:

$$R = R_{bb} + \frac{X - X_{bb}}{G} + Q$$

with : $G = (X_{bb} - X_{sp}) / (R_{bb} - R_{sp})$
$Q = u.(X - X_{bb})(X - X_{sp}) / G^2$

R is the radiance corresponding to X numeric counts associated to Earth observation. Introducing the G and Q expressions in R formulation, one can deduce a direct relation between R and the corresponding numeric counts X:

$$R = a_2 X^2 + a_1 X + a_0$$

The identification of the different terms gives:

$$a_2 = \frac{u}{G^2} \qquad a_1 = \frac{1}{G} - u\frac{X_{sp} - X_{bb}}{G^2} \qquad a_0 = R_{bb} - \frac{X_{bb}}{G} + u\frac{X_{bb} X_{sp}}{G^2}$$

These calibration coefficients are stored in the level1b *amsual1b*, *amsubl1b* and *mhsl1b* files. The nonlinearity coefficients (*u*) are referenced in the parameters files *amsua_clcoefs.dat*, *amsub_clcoefs.dat* and *mhs_clcoefs.dat*. The radiances are converted into brightness temperatures using the inverted Planck's law. These results are reported in the level1c file.

8.3.9. Detection/correction of moon contamination in AMSU-B and MHS (amsubcl/mhscl)

The four space view samples of AMSU-B and MHS are taken at different scanning angles, separated by 1.0° and 1.11° respectively. Consequently when the moon passes close to the space views the four samples are affected differently. (The moon subtends an angle of ~0.5°). For AAPP version 4 and earlier no account is taken of this, and the calibration is normally rejected by quality control – since the difference between the space view counts exceeds the permitted tolerance. For AAPP version 5 we compute the angle between the moon and each of the four space view samples, rejecting those samples for which the angle is less than a threshold defined in *amsub_clparams.dat* or *mhs_clparams.dat* (nominally 2.0°). If all samples are within this threshold then we use the single sample with the lowest counts value.

The method of computing the moon angles is the same as that described in section 8.3.10.

8.3.10. Detection/correction of moon contamination in AMSU-A (ATOVIN)

In the reference frame of the fixed stars the AMSU-A space view traces a fixed circle once per orbit, with radius typically 7 degrees. When the moon crosses this circle the space-view antenna temperatures are perturbed by up to 2 K for approximately 10 minutes per orbit. This leads to calibration errors. The errors are not detected by the quality control procedures in AMSUACL, and the level 1b format (prior to NOAA-N) makes no provision for flagging moon contamination. Therefore a correction is applied at level 1c. (The NOAA-N 1b format does make provision for flagging moon contamination, but for AAPP-5 and later we use the same method as AAPP-4.)

The right ascension and declination of the moon are first calculated at the start and end of the data period using a standard astronomical formula, and are interpolated for intermediate times. The formula implemented has an accuracy of ±0.3 degrees.

For each scan the latitude and longitude of the two Earth samples closest to nadir are used to establish the local azimuth of the instrument scan axis. The space view elevation is a fixed instrument parameter. The local sidereal time of the moon is then computed given the observation time, latitude and longitude. Hence the angular separation between the moon and the space view is computed. If the angular separation exceeds a preset threshold then moon contamination is deemed to have occurred and flags are set. Since AMSU-A1 and AMSU-A2 may use different space view angles the calculation needs to be performed for each instrument.

The moon contamination may be corrected as follows:

Using the supplied calibration coefficients, compute the radiometric counts at nominal space and warm target temperatures (i.e. the inverse of the calibration procedure outlined in section 5.3.7) and hence the channel gains. Also compute the nonlinearity parameter.

Interpolate the gains across the period of the contaminated data. A linear interpolation is implemented.

Compute the corrected calibration coefficients assuming that the warm calibration counts and nonlinearity parameter are still valid.

By interpolating the gains rather than the calibration coefficients themselves we ensure that the calibration is not significantly degraded for warm scenes (i.e. close to the internal target temperature), and that the interpolation errors are minimised for cooler scenes.

8.3.11. Scan-dependent correction due to non-unity antenna reflectivity (ATOVIN)

This correction is implemented for MHS in AAPP version 5 onwards. It is desirable in view of the fact that MHS uses a different polarization for channels 18 and 19 compared with AMSU-B.

AMSU and MHS use a 45° antenna that rotates relative to the plane of polarisation of the receiver. Let the antenna reflectivities for electric fields parallel and perpendicular to the plane of incidence be $R_{//}$ and $R_{\perp}$. From electromagnetic theory we expect $R_{\perp}$ to be larger than $R_{//}$.

The net reflectivity varies as the antenna rotates, according to

$$R_{\theta} = R_{0°} \cos^2 \theta + R_{90°} \sin^2 \theta \tag{1}$$

where we define $\theta = 0°$ at nadir.

For AMSU-B, all channels have V polarisation, i.e. at nadir the electric field is perpendicular to the plane of incidence ($R_{0°} = R_{\perp}$, $R_{90°} = R_{//}$). AMSU-A and MHS have some H-polarisation channels.

The antenna temperatures for Earth view, space view and black-body view (t_E, t_{SP} and t_{bb}) are given by

$$
\begin{aligned}
t_E &= (1 - R_{\theta}) T_{REF} + R_{\theta} T_E \\
t_{SP} &= (1 - R_{SP}) T_{REF} + R_{SP} T_{SP} \\
t_{bb} &= (1 - R_{bb}) T_{REF} + R_{bb} T_{bb}
\end{aligned} \tag{2}
$$

where T_{REF} is the temperature of the antenna reflector and T_E, T_{SP} and T_{bb} are the true brightness temperatures. (For clarity we are using brightness temperatures rather than radiance).

The calibration process described in section 8.3.8 derives a calibrated Earth-view brightness temperature, B_E, that is a linear function of the antenna temperature. (For a linear detector the antenna temperature is a linear function of instrument counts). So,

$$B_E = \frac{t_E - t_{bb}}{t_{bb} - t_{SP}} \times (T_{bb} - T_{SP}) + T_{bb}$$

For a non-ideal antenna we substitute for antenna temperatures (equ 2) to give

$$B_E = \frac{R_{\theta}(T_E - T_{REF}) - R_{bb}(T_{bb} - T_{REF})}{R_{bb}(T_{bb} - T_{REF}) - R_{SP}(T_{SP} - T_{REF})} \times (T_{bb} - T_{SP}) + T_{bb}$$

Now the reflector temperature is not explicitly measured, but is approximately equal to the temperature of the calibration black body, so

$$B_E \quad \frac{R_{\theta}(T_E - T_{bb})}{R_{SP}} + T_{bb}$$

and the correction to the measured brightness temperature is

$$\Delta T = T_E - B_E = (T_E - T_{bb})\left(1 - \frac{R_{\theta}}{R_{SP}}\right)$$

Substituting the angular dependence of reflectivity (equ 1) gives (after some trigonometric manipulation)

$$\Delta T = \alpha \left(T_{bb} - T_E \right) \left(\cos 2\theta_E - \cos 2\theta_{SP} \right) / 2 \qquad (3)$$

where $\alpha = 1 - \dfrac{R_{90°}}{R_{0°}}$

For V-pol channels $\alpha = 1 - \dfrac{R_{//}}{R_{\perp}}$ – giving a positive correction if $T_{bb} > T_E$. For H-pol channels the sign

of the correction is reversed.

The values of α for the different channels can be derived from pre-launch radiometric calibration tests – from the brightness temperature error when the Earth target (in nadir) is close to the temperature of the space target.

Values of α for MHS are held in file *fdf.dat*. For a typical atmospheric scene, applying the correction changes the channel 19 minus channel 20 brightness temperature difference by up to 0.2K. For AMSU-B the error is similar for all channels, though the correction could be implemented if required simply by adding the antenna coefficients to *fdf.dat*.

8.4. DATA INGEST FOR FILES IN BUFR, HDF5 OR EPS FORMAT

AAPP allows the ingest of certain types of external data that are already calibrated, and are supplied in a standard format such as BUFR, HDF5 or EPS level 1. For example, files transmitted in near-real-time via EUMETCast, or available from the EUMETSAT Data Centre or the NOAA "CLASS" archive. These are listed in Table 5.

Table 5: Ingest of external level 1 datasets

Satellite	Instrument	Level	Format	Processing script	Output
MetOp	AMSU, MHS, HIRS, IASI	Level 1	BUFR	aapp_decodebufr_1c	AAPP 1c
MetOp	AVHRR	Level 1	EPS	convert_avh1b	AAPP AVHRR 1b (pseudo)
NPP	ATMS, CrIS	SDR	BUFR	aapp_decodebufr_1c	AAPP 1c
NPP	ATMS, CrIS	SDR	HDF5	atms_sdr, cris_sdr	AAPP 1c
FY-3	MWTS, MWHS, IRAS, MWRI	SDR	HDF5	mwts_sdr, mwhs_sdr, etc.	AAPP 1c

Note that the AVHRR 1b file listed above is created in the AAPP format, but it does *not* contain instrument counts, it contains 16-bit (or optionally 10-bit) scaled radiances. These need to be multiplied by the scaling factors that are found in the fields normally used to hold the calibration coefficients (i.e. avh_calvis, avh_calir).

In the case of MWHS and MWTS, the AAPP ingest includes some additional quality control measures that were found to be necessary when the data were first evaluated, including:

- Time stamp consistency check
- Navigation consistency check
- Examination of the calibration quality flags
- Consistency check of the consistency of the antenna position counts for cold and warm calibration views
- Flagging of lunar contamination of the space view
- Consistency check of the calibration gain (only necessary for MWTS)

Any samples that fail these checks have the radiances set to "missing". It is likely that over time the data provider will implement additional quality checks, but the AAPP checks may still prove useful. See source code of subroutines mwts_sdr_out.F and mwhs_sdr_out.F for full details.

8.5. PREPROCESSING AND MAPPING

Mapping one sounder to the grid of another is performed by the module **ATOVPP**.

Mapping of the imager AVHRR to HIRS grid is performed by the module AVH2HIRS.

This chapter describes pre-processing (made before and after mapping), LUT map production and then mapping. The end of this chapter describes suggestions for **ATOVPP** customization (e.g. adding new mapping).

After processing, 1D level files will be created.

This document outlines scientific aspects of **ATOVPP**. It describes the pre-processing of the different ATOVS instruments. It details the strategy used when selecting fields-of-view from one instrument to map to another.

The **ATOVPP** 'fixed data files' for each instrument define many of the corrections, coefficients and thresholds used in the pre-processing. Such files are largely described in corresponding software documentation and are provided with software, but can be modified and implemented for users' needs.

8.5.1. Pre-processing

Pre-processing is done for sounders in **ATOVPP**. As they are principally made before mapping, in this documentation if nothing is specified, it means that pre-processing is made before mapping. If pre-processing is made after mapping it is explicitly mentioned. Values given in the text below are for illustration and may differ from those used.

General pre-processing for all sounders

All the instruments share certain elements of pre-processing.

BIAS CORRECTIONS :

These are added to the brightness temperatures (level 1C) before any other processing takes place. They depend on channel and scan position. If values are not provided in the instrument 'fixed data file' then values of zero are used. Actually this correction is only made for mapping MSU to HIRS.

SURFACE TYPE :

Surface information comes from a land/sea bit mask on a 1/6th degree by 1/6th degree lat/lon regular grid (this mask used topographic data from an ITPP atlas stored in file '*mapbitls.dat*'). Surface type is found by examining all grid points within a box centred on the instrument field-of-view (fov) and approximately the same size as the fov. The fov is classed land (or sea) only if every point in this box is land (or sea). Otherwise, the surface type is 'mixed'.

If either latitude or longitude are out range then values of -999999 are returned for surface type.

SURFACE ELEVATION :

Surface elevation information is stored in '*maptopog.dat*' file, similar to the one described above (1/6th degree by 1/6th degree lat/lon, heights in 100s of feet). Height provided is that for the nearest point in the grid, and is zero for spots over the sea. If either latitude or longitude are out of range then values of -999999 are returned for surface type.

HIRS pre-processing

No further pre-processing of HIRS is done.

AMSU-A pre-processing

The aim is to define if there is a cloudy/precipitation situation and if the surface type detected from data can influence inversion processing. The two main tests are the scattering index and the surface and cloud cost function. Other tests have also been coded.

*Note :*Some pre-processing on the AMSU-A grid uses mapped brightness temperatures from AMSU-B. This mapping is done within the AMSU-A pre-processing, and is described below in the section on mapping.

SCATTERING INDEX :

Theory:

Typical atmospheric hydrometeors have sizes around 0.01mm for liquid cloud drops and 0.1mm to 1mm for drizzle and rain drops. Ice crystals are similar in size to rain drops, although exceptionally snowflakes and ice aggregates associated with large cumulus can reach sizes of 10mm. Mie theory, which is generally applicable at these wavelengths, predicts that when the wavelength of observation is long compared to the hydrometeor size, scattering is negligible. For most rain and ice hydrometeors scattering processes become important at wavelengths below around 5mm (frequency > 60 GHz). Absorption remains significant for wavelengths up to 20mm (15 GHz). Therefore rain and ice is characterised by absorption in AMSU channels 1 to 14 (24-57 GHz) and by scattering in AMSU channels 15 to 20 (89 to 190 GHz). In the absence of scattering-sized hydrometeors, absorption by

smaller hydrometeors will become the dominant radiative process at higher frequency. In the presence of large hydrometeors, scattering may be significant at 50 GHz.

We use this property to compare a prediction of channel 15 brightness temperature based on channels 1, 2 and 3, assuming no scattering hydrometeors, with that observed for channel 15. In the absence of scattering hydrometeors, the agreement will be within 5K. As the population of scattering hydrometeors increases the higher frequency observation will cool and a large difference between observation and prediction will result. This difference is our scattering index, and a simple threshold can be applied to detect scattering hydrometeors. These hydrometeors will contaminate the temperature sounding channels around 50 GHz sufficiently to prevent their use.

In AAPP the scattering index method has only been applied over the sea. Over land surfaces hydrometeor scattering is very obvious but some surfaces (snow, ice, desert) can give scattering signatures. Until we are confident we can separate surface and atmospheric scattering, the method should only be used over the sea. Scattering index is calculated for other surfaces but using coefficients appropriate for the sea and therefore gives erroneous results.

There are known problems with this technique. Firstly it makes no allowance for an emission brightband. Some ice particles, when they melt, create paths of liquid water through the crystal which will absorb radiation strongly because of their length. If sufficient melting snow particles are present the absorption becomes very strong and the brightness temperatures are raised. These types of low density snowflakes do not scatter strongly, and so this warm emission will not be masked. In this case, brightness temperatures will be elevated in all channels, and some contaminated data could give a scattering index of zero. Therefore additional tests are needed, which work by flagging strong emission. It is also possible to get a scattering brightband when ice particles are thinly coated with water. This creates a particle with an effective dielectric property that makes it appear like a much larger particle to the incident electromagnetic wave. If this happens scattering is enhanced, in an identical way to weather radar brightband. This problem is most serious at low frequency.

Method :

Compute scattering index. This consists of estimating AMSU-A channel 15 brightness temperature from channels 1, 2 and 3, and then determine scattering index as : Estimated TB15 - Observed TB15

AMSU-A channel 15 brightness temperature is estimated as :

$ETB15 = a + b*TB1 + c*TB2 + d*TB3$

where TB1, 2 and 3 are the observed brightness temperatures in channel 1, 2, 3 and ETB15 is the estimated channel 15 value. Coefficients a, b, c and d are third order polynomials in the secant of the zenith angle (z):

$a = a_0 + a_1 x + a_2 x^2 + a_3 x^3$, where $x = \sec(z)-1$

and similarly for b, c, d. The coefficients (a_0, a_1, etc.) are provided in data file AMSUA.fdf and were originally derived from a clear-air dataset over ocean.

Scattering index is then :

$SI = ETB15 - TB15$

We flag fovs where SI > 10K, i.e. where the BT predicted from the low frequencies is significantly warmer than the actual channel 15 BT.

Note : this pre-processing is also made, after mapping, on AMSU-A brightness temperature mapped to HIRS grid.

RANGE OF AMSU-B 89 GHZ :

Theory:

We can use the high spatial resolution of the AMSU-B instrument to look for inhomogeneous 89GHz values within the AMSU-A footprint. The variables we will attempt to retrieve have much larger spatial scales than those we attempt to preprocess. If there are inhomogeneities, these are most likely due to contamination by one of a number of possible causes, all of which we would like to flag in the preprocessor.

Method:

Calculate the range of the AMSU-B 89 GHz channel over the AMSU-A footprint within the mapping (routine PPB2A). Flag the AMSU-A fov when the range exceeds 12K.

ESTIMATE SURFACE TYPE AND DEEP LIQUID WATER CLOUD DETECTION:

Theory:

To estimate surface type from the brightness temperatures, we use a minimum variance scheme. Mean brightness temperatures and BT covariance matrices have been calculated (with a radiative transfer model) for the 20 AMSU channels for different surface types, with no cloud liquid water. For each surface type (vector TBM, matrix C) we evaluate the cost function:

$$J = (TB - TBM)C^{-1}(TB - TBM)^T$$

where TB are the observed brightness temperatures. The surface type is identified as that minimising *J*. If the surface type is sea and if *J* is larger than a threshold value (normalised by number of channels squared) then we set a flag to indicate cloud liquid water may be present.

Method:

This has been installed but the coefficients are not well developed and its results are currently not very meaningful.

We use only selected channels: 1, 2 and 3

Eight surface types are determined:

1 = Bare young ice (i.e. new ice, no snow)

2 = Dry land (i.e. dry with or without significant vegetation)

3 = Dry snow (i.e. snow with water less than 2%, over land)

4 = Multi-year ice (i.e. old ice with snow [assumed dry] cover)

5 = Sea (i.e. open water, no islands, ice-free, wind < 14 m/s)

6 = Wet forest (i.e. established forest with wet canopy)

7 = Wet land (i.e. non-forested land with a wet surface)

8 = Wet snow (i.e. snow with water content > 2%)

Note : If surface type is 1, 4 or 8 and channel 1 > 275 K surface type is set to

9 = Desert.

Flags are set if:
- the minimum cost exceeds the cloud-test threshold (sea only)
- the estimated surface type incompatible with topography

- the surface type is one where the emissivity is highly variable (2, 3, 6, 7 and 9)

Note : this pre-processing is also made, after mapping, on AMSU-A brightness temperature mapped to HIRS grid.

CLOUD CATEGORIES :

For the purposes of further processing, we class the fov as contaminated if it is flagged for precipitation/scattering by any of tests described above.

Similarly we consider it contaminated if it is flagged in the preceding test for incompatible surface types, or with a surface type that we cannot use.

If the fov is not contaminated but cloud liquid water has been detected (using the cost function technique) then the fov is considered 'cloudy'.

If the fov is neither 'contaminated' nor 'cloudy' then we call it 'clear'. This means only that we detect no cloud in the microwave. There may be cloud present that would affect the infra-red.

As a rough guide clear means the cloud LWP is less than 100 gm-2, cloudy means the LWP is less than 500 gm-2. Higher values of LWP, whether or not combined with precipitation, ice cloud or mixed surface are classed as contaminated. A substantial percentage of the world's extensive stratocumulus sheets will have LWP less than 50 gm-2, and 500 gm-2 will rarely be exceeded outside major tropical or middle latitude storm systems, or in deep convection.

EXISTING BUT REDUNDANT CODE :

* CROSBY logistic precipitation test :

Theory:

The theory comes from Crosby, Ferraro & Wu [6]. This test, also uses the relative scattering by hydrometeors at high frequency to flag rain or deep ice cloud. The information is very similar to the scattering index and so this test may be redundant.

Method:

Probability of rain is calculated as :

$$P = 1 / (1 + e^{-f})$$
$$\text{where} \quad f = 10.5 + 0.184*TB1 - 0.221*TB15$$

We flag the fov when probability of rain > 0.05

Note : this pre-processing is also performed, after mapping, on AMSU-A brightness temperature mapped to HIRS grid.

* GRODY light rain test :

Theory:

This method is a simple adaptation of a rainfall algorithm for SSM/I to the AMSU-A frequencies [10]. It will be triggered by strong absorption and so should flag deep liquid water cloud or an emission brightband (see earlier discussion). Note NOAA/NESDIS have developed their tests further.

Method:

Estimated channel 1 brightness temperature (ETB1) is computed as :

$$ETB1 = 38 + 0.88 \cdot TB2$$

If observed TB1 < ETB1 then set a flag. Note that presently we do not act on this flag as we expect the scattering index test to flag all such cases.

Note : this pre-processing is also made, after mapping, on AMSU-A brightness temperature mapped to HIRS grid.

AMSU-B or MHS pre-processing

MEDIAN FILTER :

Theory:

Spikes in the 89GHz field may reveal contaminated data (e.g. due to scattering).

Method:

For each AMSU-B (or MHS) fov, find the median value of 89 GHz brightness temperature in the surrounding box of 3x3 fovs (routine **median**). Flag the central fov if it differs by more than 10 K from central value. Note that we do not act on this flag in mapping AMSU-B (or MHS) to AMSU-A.

SCATTERING INDEX :

This pre-processing is made after mapping. It presumes that we have mapped AMSU-A brightness temperatures. Recalculate AMSU-A scattering index using AMSU-B (or MHS) 89 GHz instead of AMSU-A. A flag is set if AMSU-A and AMSU-B (or MHS) 89 GHz channels differ.

CIRRUS TEST :

This pre-processing is made on full resolution unmapped AMSU-B (or MHS) data. It assumes AMSU-A data have been mapped to AMSU-B (or MHS). It therefore assumes that the AMSU-A fov is homogeneous. Otherwise the concept is identical to the AMSU-A scattering index (see AMSU-A preprocessing scattering index). Recalculate AMSU-B (or MHS) 183±7 GHz (AMSU channel 20) using AMSU-A channels 1 and 2 and AMSU-B (or MHS) 89 and 150 GHz. A flag is set if the recalculated AMSU-B (or MHS) 183±7 GHz value differs from the observed value.

$$ETB20 = a + b \cdot TB1 + c \cdot TB2 + d \cdot TB16 + e \cdot TB17$$

where TB1, 2, 16 and 17 are the observed brightness temperatures in channel 1, 2, 16 and 17 and ETB20 is the estimated channel 20 value. Coefficients a, b, c and d are third order polynomials in the secant of the scan angle.

Scattering index is then:

$$SI = ETB20 - TB20$$

We flag fovs where SI > 10 K, or < -10 K.

NWC-SAF SCATTERING AND PRECIPITATION TEST :

This test was supplied by Ralf Bennartz and was developed for the Nowcasting and Very Short Range Forecasting Satellite Application Facility (NWC-SAF). Full details are provided in reference [25]

A scattering index is computed based on AMSU-B channels 16 and 17, and AMSU-A channel 1. The index is defined as:

$$S_{l1} = (T_{89} - T_{150}) - (0.158 + 0.0163\theta)$$ AMSU-B land, AMSU-A water or coast

$$S_{l2} = (T_{23} - T_{150}) - (-1.7428 + 0.0776\theta)$$ AMSU-B land, AMSU-A land

$$S_{s1} = (T_{89} - T_{150}) - (aveseaback + 0.11\theta)$$ AMSU-B sea

$$S_c = (1-l)\, S_{s1} + l\, S_{l1}$$ Coast

where θ is the zenith angle in degrees, l is the land fraction in the AMSU-B footprint and *aveseaback* is the average background temperature difference between 89 and 150 GHz over the ocean, computed over the local area.

Based on the scattering index, a likelihood of different intensity classes of precipitation is calculated, using look-up tables. These classes are given below:

Class	Type of precipitation	Min rain rate (mm/h)	Max rain rate (mm/h)
1	No precipitation	0.0	0.1
2	Risk of light precipitation	0.1	0.5
3	Light/moderate	0.5	5.0
4	Intensive	5.0	∞

The precipitation likelihoods are only computed if the scattering index is between –20K and +100K.

MSU pre-processing

LIMB DARKENING

Limb darkening is the effect under which brightness temperatures (especially in channel 1) are cooler at the edge of the scan than at nadir. The effect increases non-linearly with scan angle, and for channel 1 depends strongly on surface emissivity.

This creates two problems in the mapping of MSU to HIRS:

we are mapping a non-linear effect linearly from coarse-resolution data

MSU doesn't extend as far as HIRS at the edge of the scan and so here we are extrapolating the limb-darkening effect

It is possible to specify 'limb-darkening curves' in the MSU fixed data file - one for land and one for sea. These are defined for each channel and for each HIRS scan angle. They represent typical differences in brightness temperature between that scan angle and nadir.

These curves are subtracted from the MSU brightness temperatures at the MSU fovs before mapping, and added back at the HIRS fovs after mapping. This may reduce errors in the mapping.

8.5.2. <u>Look up tables</u> :

This section is applicable to AMSU, MHS, HIRS, IASI and AVHRR. It is not applicable to ATMS/CrIS or to MWHS/MWTS.

Introduction

Mapping is the process of calculating a representative value for the data of one instrument (the `mapping' instrument) at the location of a field of view (fov) of a second instrument (the `target' instrument).The process of mapping can be considered as two separate steps:

- *collocations* :identify mapping fovs `close to' the target fov
- *estimations* :calculate representative values of the mapping data at the target fov, using results of the collocation (weights)

The fields of view of the two instruments create a pattern that repeats at regular intervals. This pattern is derived and then stored within a look-up-table (LUT) which provides the collocation information.

Creation of LUT, which will identify those mapping fovs which are 'close to' (collocated with) target fovs is made by subroutine **lutmap**. The LUT also provides a weight for each mapping fov for each mapping mode (nearest neighbour, bilinear interpolation, spatial average) to be applied to the BT of each collocating mapping fov to provide the mapped value.

An appropriate LUT must be produced before running mapping routines.

Collocation

The pattern created by the fovs of the mapping and target instruments is modelled on a `satellite' grid. This is defined by an axis given by the track of the sub-satellite point on the Earth's surface and an axis perpendicular to the first representing an `instantaneous' scan line at some `origin' time (say the time of the first target scan line). Displacement along the track axis is given by the time elapsed since the origin time and displacement along the scan axis is given by the scan position and the scanning geometry of the instrument.

Calculations assume:

- 'nominal' geometry (i.e. satellite and instrument characteristics are as given in a NESS107 type document [1])
- the Earth is spherical and non-rotating

Fovs of the mapping instrument are assumed to be point sources which fall either within ('collocated with') or outside of a target fov ellipse determined by the 'beam width' of the instrument. (Note that a multiplier can be applied to the beam width to increase the ellipse size and encompass a greater number of mapping fovs.).

A convenient `pattern repeat time' (LUT duration) is 32 seconds because in this period there will be exactly 192 AVHRR lines, 5 HIRS lines, 4 AMSU-A lines and 12 AMSU-B lines.

The choice of `first' lines for line numbering purposes can be quite arbitrary. There is however an advantage in choosing specific first lines, for instance in the mapping of AVHRR to HIRS. If the first HIRS line is taken to be that line started in the first TIP minor frame zero, and the first AVHRR line that line which is within the HRPT frame containing the TIP minor frame, then past monitoring

suggests that the time difference between the lines will be very stable. Similar stability would be expected between `first' lines of other instrument pairs, perhaps also using `synchronisation' with the first TIP minor frame zero to define the lines.

Empirical corrections

CONE ANGLE

Ellipse footprints are constructed on the satellite grid for each target fov. Those mapping fovs which fall inside a target fov footprint are taken to be collocated with the fov. The ellipse for target fovs can be artificially increased in size to capture a reasonable number of mapping fovs. This is done by applying a multiplication factor to the nominal cone angle.

TIME/ANGLE ADJUSTMENTS

The assumption stated above of 'nominal' geometry for deriving a LUT will be in error to a greater or lesser extent. Corrections for such errors can be made by empirical adjustment of the scan angle and time of target fovs. Note that because of the design of the AMSU instruments, up to 4 sets of corrections may be necessary for each satellite when mapping to/from an AMSU grid. However it is anticipated that such corrections will only be necessary where the size of the correction is similar to the resolution of the mapping instrument, i.e. when mapping AVHRR data.

Estimation :

The information provided by the collocation step will allow a variety of estimating algorithms to be applied :

- select nearest neighbour
- bi-linear interpolation using the four 'surrounding' mapping fovs
- spatially weighted average (gaussian function or linear)
- Backus-Gilbert convolution (AMSU-B (or MHS) to AMSU-A only)

A weight is assigned to each mapping fov for each mapping mode (nearest neighbour, bilinear interpolation, spatial average). The appropriate weight will be applied to the BT of each collocating mapping fov to provide the mapped value. A rank of the distance from the target fov is also assigned to each mapping fov (1-14, 1=shortest distance).

For the Backus-Gilbert convolution method for mapping AMSU-B (or MHS) to AMSU-A, weights are pre-calculated (routine **ppbginit**) and there is no reliance on **lutmap**.

The Look-Up-Tables

Subroutine **lutmap** returns the LUT for any mapping as a four-dimensional array. Dimensions three and four are the fov and line number of the target fov.

The identification of the mapping fovs close to a target fov is done by locating each mapping and target fov on a 2-dimensional rectangular grid of which one axis represents the track of the sub-satellite point on the Earth's surface and the other axis represents an 'instantaneous' scan line at some origin time (in practice the origin time is taken to be the start time (fov 1 time) of the target line designated 'line 1'). Displacement in the along track direction is a function of time and displacement in the along scan direction is determined by the scanning geometry of the instruments (note displacements are distances along the curved Earth's surface).

Note that the pattern of target/mapping fovs will repeat at regular intervals so the LUT only has to cover this 'pattern repeat' time. The generation of the LUT is based on 'nominal' geometry i.e. satellite and instrument characteristics are assumed to be as given in a NESS 107 type document [1]. Actual characteristics may be systematically different from these. The effect of these differences can be investigated and the results incorporated into a correction for the position of each target fov across the scan. The correction is in the form of small increments assigned to the time of the fov and to the scan angle assigned to the fov (note these corrections are believed only to be important when mapping AVHRR to HIRS (or to some other instrument) where the size of the corrections is similar to the resolution of the AVHRR instrument).

An example of a LUT entry for a target fov is shown below for mapping a sounder

818	1523	0	0	0	0	0	0	0	7
8	15	-1115	-962	1	65	94	0	0	0
8	16	3732	-829	2	19	4	0	0	0
9	15	-1115	4291	3	12	1	0	0	0
9	16	3732	4424	4	4	0	0	0	0
8	14	-5982	-1095	5	-1	0	0	0	0
7	15	-1115	-6216	6	-1	0	0	0	0
7	16	3732	-6083	7	-1	0	0	0	0
0	0	0	0	0	0	0	0	0	0
0	0	0	0	0	0	0	0	0	etc.

Table 6: LUT entry for a target fov for mapping a sounder

There are 10 elements per line and the first ten lines are shown here.

- Line 1 elements 1 and 2 give the position of the target fov within the mapping fovs as a mapping line/spot position (*100) i.e. in the example the fov is at mapping line 8.18 and mapping spot 15.23
- Line 1 element 10 gives the number of mapping fovs collocating with the target fov. In this example there are seven, and lines 2 to 8 provide information on each of these 7 collocating mapping fovs:
- Elements 1,2 give the line/spot of the mapping fov
- Elements 3,4 give the scan/track position (km) of the mapping fov relative to the target fov (*100), i.e. the first mapping fov is displaced 11.15 km to the 'left' of the target fov and 9.62 km 'below' the target fov
- Element 5 gives the ranking of the distance of the mapping fov from the target fov (1 is the nearest).
- Elements 6,7 give the weights (*100) for the fov to use in the mapping (-1 indicates that the fov takes no part):
  - 6 is the weight to be used for bi-linear interpolation
  - 7 is for spatial averaging
- Elements 8,9,10 are spare and can be used for further alternative mapping options.

A target fov LUT entry for mapping AVHRR data have a different structure:

16278	147344	21
153	1470	1477
154	1467	1480
155	1465	1481

156	1464	1483
157	1463	1484
158	1462	1484
159	1462	1485
160	1461	1485
161	1461	1486
162	1461	1486
163	1461	1486
164	1461	1486
165	1461	1485
166	1462	1485
167	1462	1485
168	1463	1484
169	1464	1483
170	1465	1482
171	1466	1481
172	1468	1479
173	1472	1475
0	0	0
0	0	etc.

Table 7: A target fov LUT entry for mapping AVHRR

There are 40 lines and 3 elements :

- Line 1 gives the position of the target fov within the mapping grid, i.e. at map line number 162.78 and map scan position 1473.44. The third element gives the number of mapping 'collocating lines'.
- Subsequent lines provide the AVHRR line number and the range of AVHRR fovs for each collocating line (number of the first and the last spot).

The basic data for mapping will normally be held in a 'level 1C' file for the mapping instrument and there will be a corresponding level 1C (or 1D) file for the target instrument data (into which the mapped data will be finally stored). Such files may contain data for the whole of a local satellite pass or the whole of one orbit of the satellite for global data. In order to process data on machines of limited memory the data in such files will be divided into blocks held in local buffers. Subroutine **lutmap** will normally be run with a 'time difference' appropriate to the line 1 times of the original 1C (or 1D) files and then used on successive blocks of data with offset values providing a link between line numbers implicit in the local buffers and the line numbers of the original 1C (or 1D) files.

Information stored in the LUT buffer :

Each target fov will have information stored against it. The amount and type will depend on whether the mapping instrument is AVHRR or another instrument. This buffer is created by subroutine **lutmap**.

Mapping instrument not AVHRR: buffer dimension is (10, 15, X1, X2) where X1 and X2 depend on the target instrument (X1 = number of fovs, X2 = number of lines). Up to 15 sets of information are allowed of 10 elements each (see description above).

Mapping instrument AVHRR: buffer dimension is (3, 40, X1, X2) where X1 and X2 depend on the target instrument (X1 = number of fovs, X2 = number of lines). Up to 40 sets of information are allowed of 3 elements each (see description above).

8.5.3. Mapping

In **ATOVPP**, six mappings are available: MSU to HIRS, AMSU-B (or MHS) to AMSU-A, AMSU-A to HIRS, AMSU-A to AMSU-B (or MHS), AMSU-A to IASI and ATMS to CrIS. Mapping AVHRR to HIRS is performed by the module **AVH2HIRS**. Mapping of MWHS to MWTS (the sounders on the Chinese FY-3 satellite) is performed outside of ATOVPP, in a standalone program **mwhs_to_mwts.**

For AMSU, MHS, HIRS and IASI, the mapping routine **ppbtmap** sets up a list of fovs from the mapping instrument that are close to the target instrument fov. The list is passed to the appropriate routine (**ppm2h/ppb2a/ppbgb2a/ppa2h/ppa2b**) to decide which fovs to use. This section describes how these decisions are made.

Mapping MSU to HIRS

Fovs with brightness temperatures derived from secondary calibration coefficients are used only if there are none available derived from primary calibration coefficients.

MSU fovs are used irrespective of surface type. However a flag is set if the surface type of any of those selected differs from that of the HIRS fov. If limb-darkening curves are used, which are significantly different for land and sea, then such fovs should be treated with caution. Another flag is set if less than four MSU fovs were used in the mapping. This is always set for HIRS fovs 1 and 56.

Mapping AMSU-B (or MHS) to AMSU-A

Again, fovs with brightness temperatures derived from secondary calibration coefficients are used only if there are none available derived from primary calibration coefficients.

Only those AMSU-B (or MHS) fovs with the same surface type as the AMSU-A fov are mapped, unless the AMSU-A fov is of 'mixed' surface type, in which case all AMSU-B fovs are mapped. Surface type refers to that returned by routine **surfelev** from the topography datasets.

Mapping AMSU-A to HIRS

This was considerably simplified from the original method, in which care was taken only to map AMSU-A fovs with the same surface type and cloud classification. The original method would often find only one suitable AMSU-A fov for each of several HIRS fovs, and so re-use it several times. The resulting mapped values were then "blotchy".

The new method chooses all nearby AMSU-A fovs with valid brightness temperatures. It takes no account of surface type and cloud in the mapping, but flags are set if the AMSU-A fovs are not of identical surface type, and if any is flagged for cloud.

The pre-processing tests (scattering index, Crosby, Grody light rain and surface estimation) described above are repeated using the AMSU-A brightness temperatures once mapped to the HIRS grid.

Mapping AMSU-A to AMSU-B (or MHS)

AMSU-A brightness temperatures for AMSU-B (or MHS) fovs are taken directly from the nearest AMSU-A fov.

Mapping AMSU-A to IASI

The method is essentially the same as mapping AMSU-A to HIRS. The same AMSU pre-processing tests are used. Because there are four IASI fields of view per scan position the mapping process is repeated four times, with different along-track and cross track offsets.

The IASI instrument is mounted on anti-vibration mounts on the spacecraft, therefore its relationship to the other instruments is not fixed. However, considering the relatively coarse resolution of AMSU it is sufficiently accurate for ATOVPP to assume nominal IASI scan geometry, and not to take account of vibration.

Mapping AVHRR to HIRS

Mapping AVHRR has not been included in the module **ATOVPP**. However this mapping is performed in HIRS ellipse by the module AVH2HIRS, following the principles described above. This mapping used the routines **lutmap** and **av_map**. In addition AVH2HIRS generates the cloud mask.

Mapping AVHRR to IASI

Mapping AVHRR to IASI is not an ATOVPP option. However AVHRR to IASI mapping is performed as part of the IASI calibration/navigation task OPS-LRS (or within the EPS Core Ground Segment in the case of global or regional data). This mapping process is required in order to accurately geo-locate the IASI sounder data (via the IASI imager). The IASI level 1c format includes a "cluster analysis" of this mapped AVHRR data, giving information on the mean and standard deviation of the AVHRR radiances for each IASI field of view, computed for up to 7 AVHRR "classes". These classes are not assigned physical meaning (i.e. the OPS-LRS software does not attempt to identify the cloud or surface type), but the results can still be useful to the user – for example the presence of several classes implies that the AVHRR field is non-uniform.

Mapping ATMS to CrIS

For mapping ATMS to CrIS a different approach is used to those described above. This is described in detail in [33]. In brief, the method uses the actual level 1c latitude/longitude values, rather than assuming a nominal scan geometry. The ATMS radiance field for each channel is interpolated to the positions of each CrIS field of view. This function is performed by subroutine **map_atms_to_cris**, within atovpp.

Mapping MWHS to MWTS

The mapping of MWHS to MWTS (i.e. the humidity sounder on FY-3 to the temperature sounder) is *not* performed within ATOVPP, it is done by a standalone program **mwhs_to_mwts**. Using the supplied latitude/longitude values, the viewing angle differences between each MWTS spot and the neighbouring MWHS spots are calculated. Then for any angles less than 2° (threshold specified in map_mwhs_to_mwts.F) the *median* MWHS brightness temperature is computed. This method

provides a measure of robustness against occasional corrupt BT values, achieves a useful noise reduction, and is independent of prior assumptions on scan geometry.

8.5.4. Suggestions for customisation

1D format

The format of output on each grid (HIRS, AMSU-A, AMSU-B or MHS, IASI) is intended to be flexible. Some parts of the format are fixed, and other parts will be customized to fit the requirements of individual centres. The AMSU-A and AMSU-B (or MHS) 1D formats may need to be expanded to accommodate extra mappings. A change in format will require changes in the **ppxouth** and **ppxoutd** routines (where x = a for AMSU-A, b for AMSU-B (or MHS), h for HIRS and m for MSU). Those routines transfer data from storage arrays to 1D records. Customized parts are labelled [user-defined] within routines and includes.

In the case of IASI and CrIS, the number of channels and Eigenvector scores to be output in the level 1d may be customized by the user.

Pre-processing tests and corrections

The initial implementation of **ATOVPP** does not attempt to correct brightness temperatures for limb effect, surface emissivity, or cloud. However there are dummy routines in place (**ppxcorr** and **pphcloud**) which could be expanded by the individual user to perform these functions.

The routines underneath **ppproc1** and **ppproc2** are intended to be customised by individual centres. **ppproc1** is for pre-processing before any mapping has been done, and **ppproc2** is for after, where the processing depends on the use of brightness temperatures from more than one instrument. The initial implementation breaks these rules slightly. AMSU-B is mapped to AMSU-A within **ppamsua1**, which makes use of the AMSU-B (or MHS) brightness temperatures to pre-process AMSU-A before AMSU-A is mapped to the HIRS grid.

Any additional fixed data needed for the pre-processing can be placed in the 'fixed data file' for that instrument and read by **ppxfdf** to be stored in **ppxfdata.h**.

Mapping

At the heart of the mapping are the routines **ppm2h**, **ppa2h**, **ppb2h**, **ppb2a** (and **ppbgb2a**), **pph2a**, **pph2b, ppa2b** and **ppa2i**. Given a target field-of-view and a list of collocated mapping fields-of-view, these routines select which mapping fovs should be used, and then derive mapped brightness temperatures and other parameters. Initially only **ppm2h**, **ppa2h**, **ppb2a**, **ppbgb2a, ppa2b** and **ppa2i** have been coded. It is thought that some centres will have rather different requirements and so will need to adapt or code their own versions of these.

Look-up tables creation, which allows the generation of a list of mapping fovs, is made by **lutmap,** called by **pplut** which determines the mapping and initialises the parameters for calling **lutmap** (see software documentation about **ATOVPP**). Subroutine **pplut** must be modified to include a new mapping.

Memory tuning

There are two parameters that may be tuned if memory limits are a problem:

- 'dT' (include file **ppparms.h**) is the size of data block to be read, stored, and processed at a time (in milliseconds). Reducing this will ease memory usage (see software documentation about **ATOVPP**).
- Subroutine **surfelev** reads the surface elevation dataset as it requires, but for efficiency does store some lines from that dataset. The number of lines 'mx_store' is a parameter defined within **surfelev** and can be reduced if required.

8.5.5. <u>IASI pre-processing</u>

Because the volume of IASI level 1c data is more than 2 orders of magnitude greater than that of the other sounders put together, ATOVPP includes several options to allow the user to reduce this volume, while still retaining as much of the useful information as possible. These options are:
1. Spatial thinning
2. Spectral thinning (channel selection)
3. Principal Components analysis

The options are described below.

Spatial thinning

Spatial thinning is controlled via the *IASI.fdf* file.

IASI has 4 detectors arranged at different viewing angles, thus full-resolution IASI data has 4 fields of view (FOV) per scan position and 120 FOVs per scan line. The user may specify that only one FOV per scan position is to be included in the level 1d output, i.e. a factor 4 reduction in the data volume. Furthermore, the user may specify that only 1 in *n* scan line is output, where n is any integer.

In order to maximize the usefulness of the data, there are various possible ways of doing the 1 in 4 thinning. Some users will want to use the FOVs most likely to be cloud free; other users might have a preference for uniform cloud; still others may prefer a regular thinning pattern. Thus the following options are provided:

> 0 = full resolution (no thinning)
> 1 = fixed detector
> 2 = the FOV with the warmest mean AVHRR I/R radiance
> 3 = the FOV with the lowest variability in the mapped AVHRR I/R radiances
> 4 = hybrid – option 2 equator-ward of a specified latitude and option 3 pole-ward
> 5 = the FOV with the warmest IASI radiance for a specified channel (typically a window channel)
> 6 = hybrid – option 5 equator-ward of a specified latitude and option 1 pole-ward
> 7 = as for option 1, except the chosen detector is changed each scan line

In many situations – and especially over ocean – the warmest AVHRR field of view is the one most likely to be cloud-free. Similarly, if the standard deviation of mapped AVHRR radiances is low then the cloud is likely to be uniform. However, where there is sea-ice or snow the warmest field of view assumption breaks down – hence the inclusion of hybrid option 4. Options 5 and 6 may be used if for any reason there is no mapped AVHRR data available.

The user is allowed to specify a "primary" thinning mode and a "backup" mode for use if there is insufficient data to use the primary mode, e.g. if AVHRR are missing.

Spectral thinning (channel selection)

Spectral thinning is controlled via the *IASI.fdf* file. This file includes a list of channels that are to be included in the level 1d output (see [28]).

The level 1d user may customize the 1d format to set the maximum number of channel slots by changing a parameter in *iasi1d.h* – and then re-compiling ATOVPP. However the channels themselves may be changed via *IASI.fdf* at any time, provided the number of channels is less than the maximum.

Principal Components (PC) Analysis

An alternative approach to spectral thinning is to compute the projection of each spectrum along a limited number of orthogonal eigenvectors. If we represent the noise-normalised spectrum as a column vector **y** (dimension *m* channels) and the eigenvectors as a column-orthogonal matrix **U** (*m* channels × *n* eigenvectors) then the vector of PC scores, **c**, is given by

$$\mathbf{c} = \mathbf{U}^{\mathbf{T}}\mathbf{y}$$

Typically 300 scores would contain most of the useful information in the original spectra. If the spectra are correctly noise-normalised then the score for a given eigenvector is equal to the signal-to-noise ratio (SNR) for detecting the presence of that eigenvector in the spectrum. For data storage purposes the scores are then quantized: in AAPP they are quantized at 0.5 SNR-unit intervals, which gives acceptably small loss.

IASI level 1c spectra are Gaussian apodised (see footnote[2]). The process of apodisation results in the noise no longer being "white" in the interferogram domain. Therefore before computing the PC scores it is preferable to "de-apodise" each spectrum back to self-apodised form, based on nominal instrument characteristics supplied to AAPP in a data file (see [27]). If this were not done then information would be lost when the scores are quantized for storage purposes. In practice, most users do not de-apodise (and the eigenvectors distributed by EUMETSAT are for unmodified level 1c spectra), therefore AAPP has been designed to accommodate either option.

AAPP also performs a check on the accuracy of the normalized radiances *y′* that are reconstructed by inverting the above equation. The "reconstruction score", *RS*, is computed for each spectra by summing over channels:

$$RS = \sqrt{\frac{1}{\text{nchan}} \sum_{i=\text{startchan}}^{\text{endchan}} \left(y_i' - y_i \right)^2}$$

The reconstruction score is computed for the three nominal IASI bands, which are Band 1 = 645.0-1210.0 cm^{-1}, Band 2 = 1210.0-2000.0 cm^{-1}, Band 3 = 2000.0-2760.0 cm^{-1}. We would expect a reconstruction score of approximately 1.0 – i.e. expect fitting errors to be of the order of instrument noise. If the value is significantly higher it implies that the fitting accuracy is poor for that spectrum. See reference [28] for a more detailed description.

---

[2] The wavenumber-domain IASI level 1c Instrument Spectral Response Function is the inverse Fourier Transform of an interferogram-domain truncated Gaussian with a cutoff at ±1.96800 cm. The interferogram-domain Gaussian function is the direct Fourier transform of a wavenumber-domain Gaussian with a full width at half height = 0.5 cm^{-1}. See reference [27]

IASI cloud tests

Several cloud tests are implemented in AAPP, with independent cloud flags for each test. Currently these are:

1. Standard deviation of IASI radiances at 2390 cm^{-1} for the 4 detectors at each scan position. If the standard deviation exceeds three times the nominal NEDT at that frequency, the cloud flag is set for that field of regard.
2. Make use of mapped AMSU (channels 4, 5 and 6) in order to simulate IASI radiance at 2390 cm^{-1}.

For more detail on these tests, see Cheng et. al., 2006, "The Use of Principal Components Analysis (PCA) in Processing Simulated IASI Data", ITSC-15, poster A17.

The data variable iasi1d_cloudflag contains the results of these tests. It is a 10-element array: elements 1 and 2 contain the test variable (e.g. standard deviation of the radiances) and element 10 contains a combined flag, 1 bit for each test.

In addition, cloud and surface parameters may be provided by EUMETSAT's ground segment, when working with global data (EPS format v8.0 onwards). The AAPP BUFR decoder stores cloud fraction in *iasi1c_GEUMAvhrr1BCldFrac* and land fraction in *iasi1c_GEUMAvhrr1BLandFrac*. Then atovpp transfers them to elements 3 and 4 of iasi1d_cloudflag.

A header variable (iasi1d_h_cloudtests) indicates which tests have actually been performed.

IASI processing external to AAPP

The user can easily re-construct Gaussian-apodised radiance spectra, **R**, directly from the PC scores:

$$\mathbf{R} = \mathbf{U}'\mathbf{c}$$

where **U'** is obtained from **U** by de-normalising (and optionally apodising). **U'** is supplied as an AAPP data file.

AAPP does not include software for the generation of eigenvectors. These will be supplied via a data file. However, for completeness the process of generating the eigenvectors is described below:

1. A set of reference spectra is assembled. These may be either real IASI spectra (post launch) or simulations (pre-launch). Typically the number of spectra used is of the of 100000.

2. The reference spectra are noise-normalised (and optionally de-apodised). Call the resulting matrix **Y** (m channels × N spectra)

3. Form the covariance matrix $\mathbf{C} = \mathbf{Y}\mathbf{Y}^{\mathrm{T}} / N$

4. Compute the eigenvectors, **U**, and eigenvalues, **Λ**, using a standard library function (such as EIGENQL in IDL): $\mathbf{C} = \mathbf{U}\mathbf{\Lambda}\mathbf{U}^{\mathrm{T}}$

5. Save the first n eigenvectors in a data file for AAPP.

8.5.6. CrIS pre-processing

CrIS pre-processing tasks closely parallel those described in the previous section for IASI. The main differences are:

- CrIS has 9 detectors (c.f. 4 for IASI)
- The CrIS 1c file does not come with imager radiances included. In the initial implementation of AAPP v7, VIIRS is not mapped to CrIS, therefore the thinning options are restricted to those that can be performed with CrIS alone.

Spatial and spectral thinning are controlled using file *CRIS.fdf*. It is possible to specify any combination of detectors to use in the output file. The following possibilities are expected to be most useful:

1. Full resolution
2. Intermediate resolution (detectors 2,4,6,8)
3. Fixed detector (central)
4. Warmest FOV (with option to use a fixed detector pole-ward of a specified latitude)

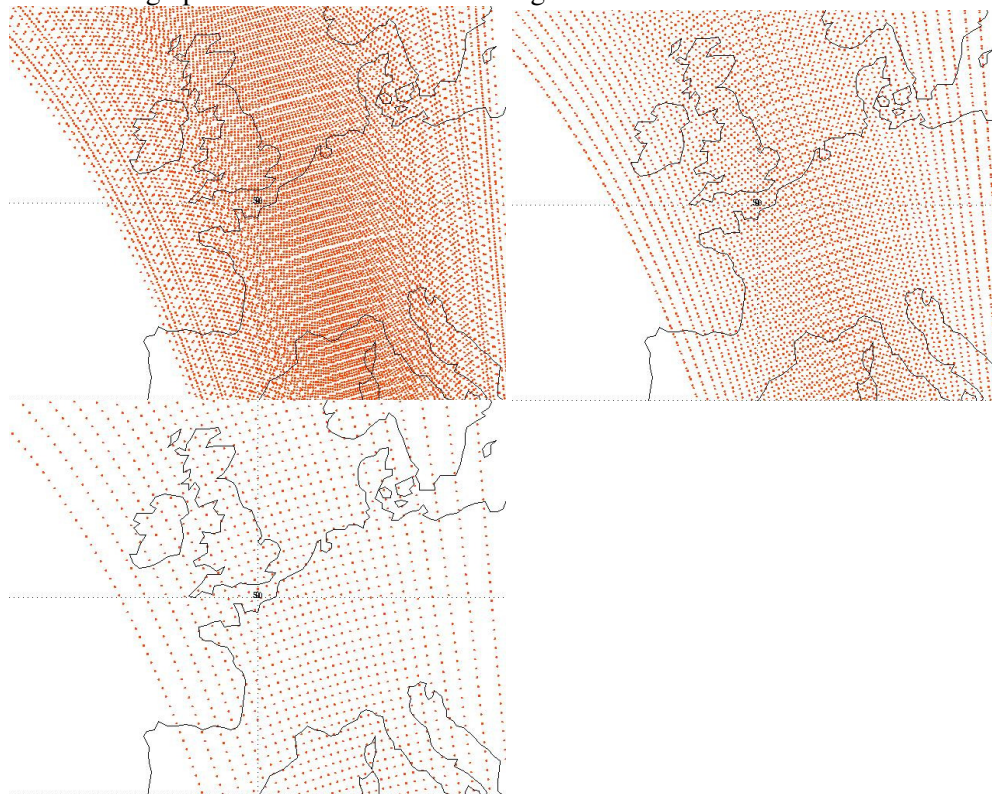The thinning options 1-3 are illustrated in Figure 10.

Figure 10: Illustration of thinning options for CrIS: full resolution (9 detectors), 4 detectors, 1 detector.

When Suomi-NPP was first launched, CrIS interferograms were transmitted to ground with the following spectral sampling intervals: band 1 – 0.625 cm^{-1}, band 2 – 1.25 cm^{-1}, band 3 – 2.5 cm^{-1}. In December 2014 this was changed to 0.625 cm^{-1} for all three bands, but the processing software retained the old sampling. For JPSS-1, the intention is to move to "full spectral resolution" by default. The AAPP ingest routines can accept either FSR or non-FSR data. Also, AAPP has a tool *cris_degrade_fsr* that can convert FSR data to normal resolution data. It uses an FFT method. This

may be useful for NWP centres that do not wish to move to FSR at the same time that NOAA make the transition.

8.6. AVHRR LOCAL CLOUD MASK

8.6.1. Introduction

Three versions of the AVHRR "MAIA" cloud mask were implemented in AAPP v7:

- MAIA2, which produced a cloud mask on the HIRS grid
- MAIA3, which produced a cloud mask on the native AVHRR grid ("AVHRR level 1d" output file)
- MAIA4, for VIIRS.

In AAPP v8, MAIA4 is used for all three applications. MAIA4 requires forecast files containing ancillary information; GFS model files are readily available from the internet and are downloaded automatically as required.

This documentation describes the cloud mask on the HIRS grid; for information on the other capabilities of MAIA4, please see [36].

The first aim of the AVHRR data processing is the description of the cloud cover within each HIRS field of view in order to help in the temperature and moisture retrieval process.

The cloud algorithm, presented in this chapter aims to determine cloudy AVHRR pixels which were used to describe the clouds within each HIRS spot. Thirteen values will be computed for each HIRS fov :

1 percentage clear AVHRR in HIRS FOV (*100)
2 surface temperature (K*100) – only computed over sea in MAIA4
3 Forecast temperature at 2m height (K*100)
4 mean AVHRR channel 3 over HIRS FOV (K*100)
5 mean AVHRR channel 4 over HIRS FOV (K*100)
6 mean AVHRR channel 5 over HIRS FOV (K*100)
7 black body coverage in HIRS FOV (K*100)
8 top cloud temperature over HIRS FOV for black body clouds (K*100)
9 standard deviation of top cloud temperature over HIRS FOV(K*100)
10 mean clear AVHRR channel 4 over HIRS FOV (K*100)
11 mean clear AVHRR channel 5 over HIRS FOV (K*100)
12 standard deviation of AVHRR channel 4 over HIRS FOV (K*100)
13 standard deviation of clear AVHRR channel 4 over HIRS FOV (K*100)

The main differences compared with MAIA2.1 are:

- Item 2: surface temperature was computed over both land and sea in MAIA2.1
- Item 3: If MAIA2.1 used climatology, this was the climatological SST
- Some of the missing values were set to zero in MAIA2.1; they are set to -9999 in MAIA4

If MAIA is *not* run (i.e. if environment variable RUN_MAIA is not set to "yes"), then the AVHRR to HIRS mapping can still be done, and the following definition is used for the thirteen values:

1. -
2. mean AVHRR channel 1 over HIRS FOV (albedo*10000)
3. mean AVHRR channel 2 over HIRS FOV albedo*10000)
4. mean AVHRR channel 3 over HIRS FOV (K*100 or albedo*10000)

5. mean AVHRR channel 4 over HIRS FOV (K*100)
6. mean AVHRR channel 5 over HIRS FOV (K*100)
7. -
8. -
9. -
10. -
11. -
12. standard deviation of AVHRR channel 4 over HIRS FOV (K*100)
13. -

The AVHRR image data used as input for the cloud detection are segmented into boxes of 38 lines by 33 pixels centred on each HIRS measurements and including the HIRS field of view. These boxes are called the working boxes.

8.6.2. AVH2HIRS mapping

The **AVH2HIRS** main program first reads the AVHRR level1b and HIRS level1d files. For each HIRS FOV over sea, it computes from the Grody model [10] the total water vapor content by using the AMSU-A channels 23, 31 and 50 GHz already mapped in HIRS level1d. It reads the forecast files of reflectance, SST and specific humidity. It creates a look-up table (see 8.6.3) and maps AVHRR data into HIRS FOV. It applies the cloud mask (MAIA) to the HIRS ellipse for contaminated pixels discrimination. The section for the cloud description of the HIRS level1d format which is not documented in the input file is then filled with the 13 output cloud parameters of the MAIA software.

8.6.3. Look up table

A look-up table (LUT) identifies those mapping fields of view (fovs) which are 'close to' (collocated with) target fovs.

The identification of the mapping fovs close to a target fov is done by locating each mapping and target fov on a 2-dimensional rectangular grid of which one axis represents the track of the sub-satellite point on the Earth's surface and the other axis represents an 'instantaneous' scan line at some origin time (in practice the origin time is taken to be the start time (time of the fov1) of the target line designated 'line 1'). Displacement in the along track direction is a function of time and displacement in the along scan direction is determined by the scanning geometry of the instruments (note displacements are distances along the curved Earth's surface).

Ellipse footprints are also constructed on the grid for each target fov. Those mapping fovs which fall inside a target fov footprint are taken to be collocated with the fov (the ellipse for target fovs can be artificially increased if required to capture a reasonable number of mapping fovs).

The pattern of target/mapping fovs will repeat at regular intervals so the LUT only has to cover this 'pattern repeat' time.

The generation of the LUT is based on 'nominal' geometry, i.e. satellite and instrument characteristics given by the documentation. Real (after launch) characteristics may be systematically different from these. The effect of these differences can be investigated and the results incorporated into a correction for the position of each target fov across the scan. The correction is in the form of small increments assigned to the time of the fov and to the scan angle assigned to the fov.

8.6.4. AVHRR cloud mask

For a scientific description of MAIA4, please see reference document **[36]:** "MAIA version 4 for NPP-VIIRS and NOAA/METOP-AVHRR", Scientific User Manual.